Environmental Earth Sciences (2022) 81:113
https://doi.org/10.1007/s12665-022-10176-4

THEMATIC ISSUE

# Spatial and temporal variation of dissolved $CO_2$ in rainwater from an arid region with special focus on its association with DIC and $pCO_2$

S. V. V. Dhanu Radha[1] · Chidambaram Sabarathinam[1] · Norah Al-Ayyadhi[1] · Farah K. Al-Ajeel[1] · Habib Al-Qallaf[1] · Adnan Akber[1]

Received: 26 May 2021 / Accepted: 3 January 2022 / Published online: 10 February 2022


## Abstract

Kuwait, being one of the leading oil producers in the world, is enriched with $CO_2$ in the atmosphere, despite the frequent dust storms. Rainwater dissolves the atmospheric $CO_2$ that acts as a carbon sink. The different sources for the contribution of $CO_2$ in an arid region like Kuwait were determined by collecting 50 rainwater samples from November 2018 to December 2019. Total $CO_2$, dissolved inorganic carbon (DIC) and $pCO_2$ calculated from the analytical values of rainwater chemistry were distributed spatially to identify the specific areas enriched with $CO_2$. Shuaiba, an industrial region, observed acidic pH (5.69) that led to the highest $pCO_2$ (388ppmV) while Ishbiliya, the residential area, had alkaline pH with the highest DIC and total $CO_2$ as 1147.9 µmole/L and 50.4 mg/L, respectively. The carbonate dust and major neutralizing ions were inferred to govern the DIC and the total $CO_2$ in rainwater. Comparing the rainwater values to that of the groundwater and the seawater reflects similar $pCO_2$ values, but the seawater has very high DIC. The biotic respiration and phytoplankton community influence $pCO_2$ at the ocean-atmospheric interface. This phenomenon alters the transfer of $CO_2$ to the atmospheric sink, thereby $CO_2$ concentration in the rain showers. The statistical analysis of the rainwater chemistry data for samples from both residential and industrial regions predominantly indicated the influence of natural than anthropogenic sources. Samples of the study area and those from different parts of the world were represented in a bivariate plot using Total $CO_2$ and ($HCO_3^-/Ca^{2+} + Mg^{2+}$) variables. It was inferred from the graph that the samples of GCC region fall in a definite range.

**Keywords** Rainwater · Kuwait · Dissolved inorganic carbon · $pCO_2$ · Total $CO_2$ · Carbonate dust

## Introduction

Carbon dioxide is the greenhouse gas that absorbs solar energy and increases atmospheric temperature by re-emitting infrared energy. Surface active constituents influencing the $CO_2$ in the atmosphere could come from oceans, landmasses, vegetation, industries, and volcanic eruptions that change the composition geographically and even seasonally. Weathering process also alters the composition of atmospheric $CO_2$. The exploitation of natural resources, excess $CO_2$ emissions and ecological hazards (Leakey 2009) facilitate the additional heat trapped in the earth's atmosphere and increase the global temperature. This increase in temperature leads to melting ice caps, rise in ocean levels and amplifies the acidic character of oceans, rainstorms and intense floods. The Intergovernmental Panel on Climate Change (IPCC) has predicted that the global surface temperature will likely increase by

This article is part of a Topical Collection in Environmental Earth Sciences on ''Recent Advances in Environmental Sustainability'', guest edited by Peiyue Li.

✉ S. V. V. Dhanu Radha
vdhanuradha@kisr.edu.kw

Chidambaram Sabarathinam
csabarathinam@kisr.edu.kw

Norah Al-Ayyadhi
nayyadhi@kisr.edu.kw

Farah K. Al-Ajeel
fajeel@kisr.edu.kw

Habib Al-Qallaf
hqallaf@kisr.edu.kw

Adnan Akber
aakbar@kisr.edu.kw

[1] Water Research Center, Kuwait Institute for Scientific Research, Kuwait City, Kuwait

2.6–4.8 °C by 2100 (IPCC 2013). Mansour et al. (2020) projected that by the end of the twenty-first century, Northern Arabian Peninsula would be warmer than Southern Arabian Peninsula. Higher temperatures are expected in Kuwait since it is located in the northeast of the Arabian Peninsula. The distribution of $CO_2$ in the mid-troposphere, a part of the atmosphere, was observed by Atmospheric Infrared Sounder (AIRS) instrument. It looks patchy with high concentrations in the northern hemisphere and low in the southern hemisphere. The $CO_2$ gas transport and distribution were controlled by the jet stream, large weather systems, and large-scale atmospheric circulations (nasa.gov 2013). About 1.5 g of $CO_2$ is produced annually in the USA has an annual uptake is 0.5 tons. The remaining contributes to the increase in atmospheric $CO_2$ and climate changes (USGA 2020). For decades, $CO_2$ emission has been accelerating. In the 1960s, the annual growth was 0.8 ppm per year, which reached 1.5 ppm in 198090 s, but now it has been exceeded above 2.0 ppm of annual rise (NOAA 2020). The average concentration of $CO_2$ was 414.7 ppm observed at NOAA's Mauna Loa Atmospheric Baseline Observatory in Hawaii (Voiland 2019), reflecting the consistent increase since pre-industrial times and earlier in May 2013 observation reported 400 ppm (Monastersky 2013). This scenario also affects economic growth, primarily due to carbon emissions (Baltimoore 2010). The driving force of climate change is due to enhanced $CO_2$ levels in the atmosphere affecting crop productivity in conjunction with increased water stress and temperature (Hoffman et al. 1986; Stinner et al. 1988; Rosegrant et al. 2006). Studies have also reported that increasing $CO_2$ levels affect plants physiology and growth rate (Ziska 2008).

The atmospheric carbon contains two different forms known as dissolved inorganic carbon (DIC) and dissolved organic carbon (DOC). The organic carbon is generally oxidized to carbon monoxide and inorganic carbon (Hallquist et al. 2009), subsequently removed from the atmosphere through precipitation (Goldstein and Galbally 2007). The process of oligomerization reactions transforms less soluble higher molecular masses, also facilitated by molecules oxidation. The oxidation process is more soluble, incorporated in nuclei condensation and removed from the atmosphere through rainfall (Hallquist et al. 2009). The role of organic carbon in the global carbon cycle models is also limited (Jurado et al. 2008). Significant gaps exist in assessing the global carbon cycles due to the influence of anthropogenic activities. The difference in emission and uptake obtains the atmospheric $CO_2$ increase (N). The emission is mainly due to fossil fuel ($E_F$) and the land-use change ($E_L$). The uptake of $CO_2$ is predominantly the oceanic ($V_O$) and the terrestrial ($V_T$) sinks. Then the net increase in Atmospheric $CO_2$ is derived as follows:

$$N = \left(E_F + E_L\right) - \left(V_O + V_T\right). \quad (1)$$

The net increase in atmospheric $CO_2$ concentration was estimated by Melinikov and Neill (2006) as 3.2 PgC/a. Thus, the photosynthetic uptake by aquatic biota, global water cycle, and atmospheric $CO_2$ combines to play a key role in $CO_2$ dynamics (Gombert 2002; Lerman and Mackenzie 2005; Iglesias-Rodriguez et al. 2008).

The warmer temperatures due to $CO_2$ emissions enhance evapotranspiration and reflect an unbalanced hydrological cycle on the earth's surface. Apart from the terrestrial sources, the ocean serves as the atmospheric sink of $CO_2$. Other significant sinks of $CO_2$ are rainwater and soil water (Liu et al. 2010). The rainwater is highly sensitive to atmospheric changes and dissolves $CO_2$ with other components like major ions, gases, minerals, trace elements, etc. (Hutchinson 1957; Carroll 1962). A numerical study in Nigeria observed that the decrease in pH significantly showed the increasing levels of $CO_2$ of rainwater. Robert et al. predicted that the pH of the rainwater would be reduced to 5.49 by 2100, considering $pCO_2$ at 25 °C and 1 atmosphere (Bogan et al. 2009). The acidity of rainwater was predicted to increase from 5.3% in 2000 to 93.7% by 2050 (Nwaeze and Ehiri 2017). The $CO_2$ emissions into the atmosphere also depend on the exchange of $pCO_2$ with the aquatic environment (Chung et al. 2018). An understanding of $CO_2$ export from the atmosphere through rainwater or gaseous exchange through sea air fluxes provides a solid base for predicting the trends of $CO_2$ in the atmosphere (Jones et al. 2003; Liu et al. 2010; Ashton et al. 2016). Therefore, the increase of atmospheric $CO_2$ can be estimated through rain deposition onto the surface.

$CO_2$ in water is at equilibrium with carbonic acid, bicarbonates and carbonates. They all represent in the form of dissolved inorganic carbon (DIC), governed by pH of the solution. $H_2CO_3$ is predominant in water with $pH < 6$; $HCO_3^-$ at the pH range of 7 to 9 and $CO_3^{2-}$ at a $pH > 10.5$ (Qian and Li 2011, 2012).

$$H_2O + CO_2 \rightleftharpoons H_2CO_3 \rightleftharpoons HCO_3^- + H^+ \rightleftharpoons CO_3^{2-} + 2H^+. \quad (2)$$

The increase in DIC reflects the contribution of inorganic carbon as $HCO_3^-$ either through carbonate dust or inorganic $HCO_3^-$ derived from the oxidation of organic carbon in the atmosphere. Studies report that the terrestrial and aquatic environment absorbs approximately half of the $CO_2$ derived by the fossil fuel emission and the remaining $CO_2$ is supplemented to the atmospheric sink (Sabine et al. 2004; Reay et al. 2007).

Climate projection models show significant warming by the end of the twenty-first century in the Middle East and North Africa (Bucchignani et al. 2018). Kuwait is one of the largest oil producers globally, hence studies have predicted

pollution due to $CO_2$ released by the operations in the oil sector (Al-Salem 2015; Al-Mutairi et al. 2017). Kuwait's long-term historical carbon dioxide emission record (World Bank Open data) reflects a steady rise in atmospheric $CO_2$. The data indicate climatic changes in Kuwait, with warmer summers extending till October. An unusual short intense rainfall event was observed during mid-November 2018, and relatively more frequent rain events were observed up to March 2019. The seawater surface and the atmospheric interface are very complex, and the exchange of $CO_2$ is studied and modeled by several researchers (Zappa et al. 2009; Turk et al. 2010). A significant buffering along the sea surface resulting from the deposition of calcareous planktons along the ocean floor (Ridgwell and Zeebe 2005) controls the sea surface carbon dynamics. The ocean surface is very dynamic, and rainfall facilitates the exchange of air-sea $CO_2$ flux, enhancing the uptake of oceanic $CO_2$ (Turk et al. 2010). Observation on long-term records reported a seasonal variation, leading to the change in the phytoplankton population. In recent decades, the plankton population has been influenced by sewage inflow, temperature variations, salinity in Kuwait Bay and the open sea environment (Devlin et al. 2019). Thus, geographically the terrestrial landscape adjoining the Bay and the open sea has experienced drastic growth in urbanization, population, and oil-based industries. This change in land use has resulted in variation of $CO_2$ in the atmosphere relating to the change in rainwater $CO_2$.

The study on the rainwater chemistry in Kuwait with few samples was carried out in 2005 (Tariq Rashid 2008) and subsequently on trace elements in rainwater during 2020 (Samayamanthula et al. 2021). Isotopic studies in rainwater have helped derive the Kuwait Meteoric water line and characterize the sources of groundwater recharge (Hadi et al. 2016). However, these studies focused only on the major ion concentration, local meteoric water line derivation, and groundwater rainwater interaction, but $CO_2$ levels in rainwater were not determined and discussed. $pCO_2$ plays a significant role in the carbonate chemistry of rainwater and governs their dissolution capacities. Therefore, the geochemical process and its relation to the saturation index of the carbonate minerals would be understood from $pCO_2$ values of water (Chidambaram et al. 2011). Therefore, this is the first baseline attempt in Kuwait to study rainwater $CO_2$ and compare it with the values of groundwater and seawater in Kuwait. The study aims to determine the dissolved inorganic components in rainwater, Total $CO_2$, DIC, $pCO_2$ and the spatial variations of these components in rainwater to industrial and residential areas.

### Study area

Kuwait is an arid country with an annual rainfall of 110, -120 mm (Samayamanthula et al. 2021). The rainfall is expected from October to December, and January to March. Atmospheric temperature varies from 45 to 50 °C (Chidambaram et al. 2020), with maximum and minimum values reported from June to August and December to February, respectively. Frequent dust storms are reported during the shift of seasons (Yassin et al. 2018). The annual evaporation rates vary from 2500 to 4500 mm in the coastal region and inland. Northwest winds, also known as Shamal winds, are the primary moisture source for rainfall in Kuwait. Observation on long-term data indicates that after 2005, a sudden change in wind direction was observed, mainly from the North. The variation in the atmospheric pressure that makes air move from high to low pressure is mainly due to a change in wind direction. Frequent sandstorms and variations in the wind are the sources for inputs of ions into the atmosphere. Meteorological parameters, such as temperature, rainfall, wind speed, wind direction, and humidity, also influence rainwater quality indirectly (Samayamanthula et al. 2021). The study area falls between 28.43° and 30.27° N Latitude, 46.57° and 48.58° E Longitude covering the sampling regions.

## Methodology

Thirty-two rainwater samples from residential regions and 18 from the industrial areas accounting for a total of fifty were collected from twelve different locations in Kuwait (Fig. 1) during the rainy season, between November 2018 and December 2019, by adopting standard procedures (Peden et al. 1979; IAEA/GNIP 2014). The samples collected from industrial regions represented KISR, Shuwaikh, and Shuaiba. The samples were filtered by 0.45 µm Millipore filter paper, immediately transferred to air-tight sterile polyethylene bottles and preserved in a cool dry place to enable high accuracy during the analyses of samples in the Water Research Center's (WRC) laboratories of the Kuwait Institute for Scientific Research (KISR). The physical, chemical, and microbiological parameters, such as alkalinity, pH, electrical conductivity, total dissolved solids, major cations and anions, total coliform, and E. coli, were determined using the standard methods (SMEWW 2017; ASTM 2009). The QC/QA procedures were adapted to the analytes as per the standard methods such as duplication, standard checks, and QC sample (Supplementary Table 1). Also, the samples were verified by the ion balance error equation for accuracy. The analytical results of the rainwater samples were considered as inputs in the PHREEQC software to determine total $CO_2$. The study also focused on $pCO_2$ and DIC, and these values were obtained using WATEQ4F (Version 4.0). The sample locations and spatial variations of the present study pH, DIC, $pCO_2$ and total $CO_2$ were mapped using Map Info professional software (Version V17.0.3). The groundwater

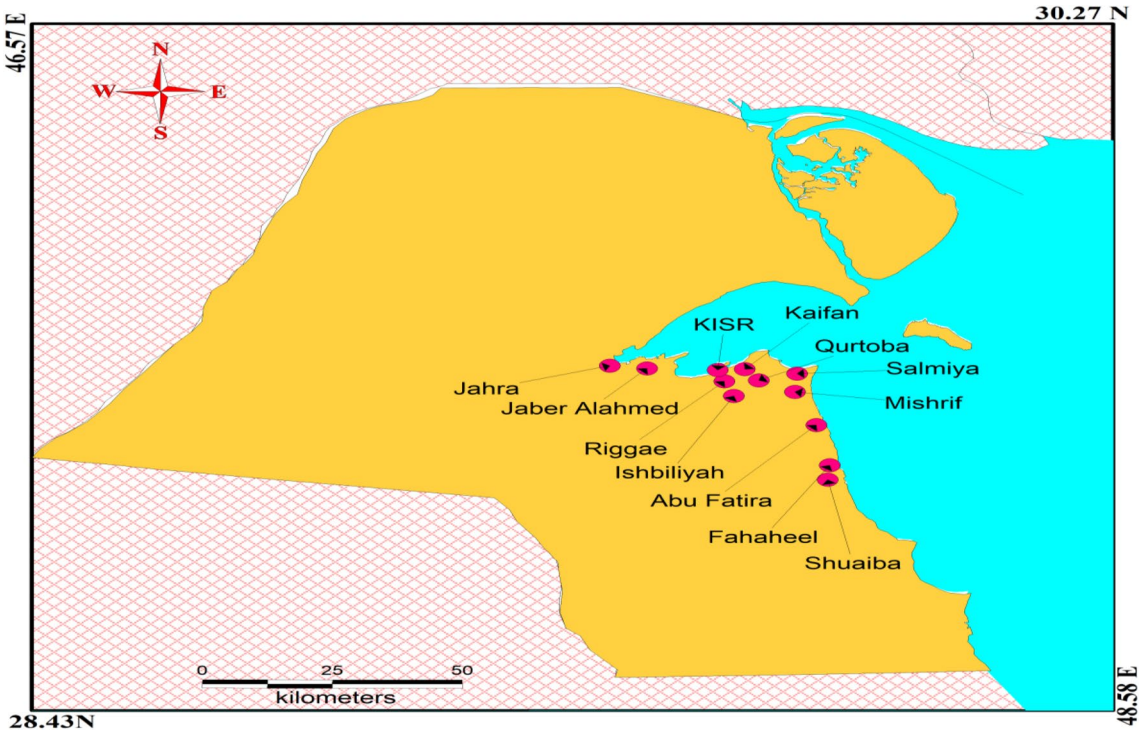


**Fig. 1** Rainwater sampling locations of residential and industrial regions

chemistry of the 113 samples analyzed in the previous study (Sabarathinam et al. 2020b) was considered to calculate the total $CO_2$, $pCO_2$, and DIC. Similarly, 20 samples collected in Kuwait Bay and the open sea environment by Bhandary et al. (2018) were utilized for seawater chemistry. These were used to calculate the above parameters (Bhandary et al. 2018).

## Results and discussion

The microbial analysis helps recognize carbon derived from microbes in rainwater as the microbes can capture carbon (Roger et al. 2018). All the filtered rainwater samples were analyzed for total coliform and E. coli. There were no detectable coliforms in the samples. A few samples were selected randomly and analyzed for the microbial parameters after filtration using different sized filters. It was observed that unfiltered samples contained total coliform and E. coli, whereas the samples filtered using 0.45 micron filter under suction ensured the complete removal of microbes. This indicates that atmospheric dust influences the microbes and enhances the dissolution of $CO_2$.

The chemistry of rainwater plays a major role in determining the amount of $CO_2$ carried by rain from the atmosphere. It varies with the area due to natural and anthropogenic activities. Studies reveal that anthropogenic input and subsequent rainwater infiltration affect groundwater quality (Wu et al. 2020; Ren et al. 2021). The electrical conductivity (EC) of the samples ranged from 16.08 to 1974 µS/cm. Bicarbonate and sulphate ions were abundant in rainwater. The average concentration of ions in the residential regions reflected the following order of dominance $HCO_3^- > SO_4^{2-} > Ca^{2+} > Cl^- > NO_3^- > Na^+ > K^+ > NH_4^+ > Mg^{2+} > NO_2^- > F^- > PO_4^{3-} > Br^-$ and in industrial region $SO_4^{2-}$ was dominant followed by $Ca^{2+}$ and $CO_3^{2-}$. The other parameters of industrial regions showed a similar relationship to that of the residential regions (Fig. 2). The alkalinity of the samples was mainly due to bicarbonates which ranged from 1.1 to 83.1 mg/L and an average of 28.80 mg/L. Samples from the KISR site in 2018 contained lower bicarbonate than samples collected in 2019 January, February, and March events. It was also noted that samples in Fahaheel contain maximum alkalinity. The pH of the rainwater samples in residential and industrial regions ranged from 5.69 to 8.21, with an average of 7.12. The samples collected during November were more acidic than samples of December, January, February, and March months. Alkaline pH was also observed in many locations (Fig. 3a). The sample from Shuaibha contains an acidic pH (5.69) due to the influence of anthropogenic sources from industrial activities (Kattan, 2020).

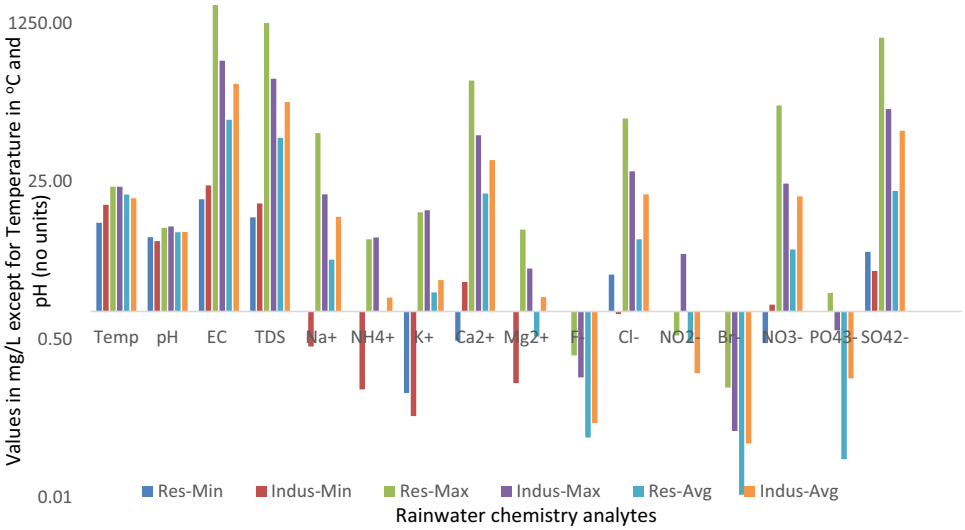


**Fig. 2** Rainwater chemistry data with minimum, maximum and average values for residential and industrial areas

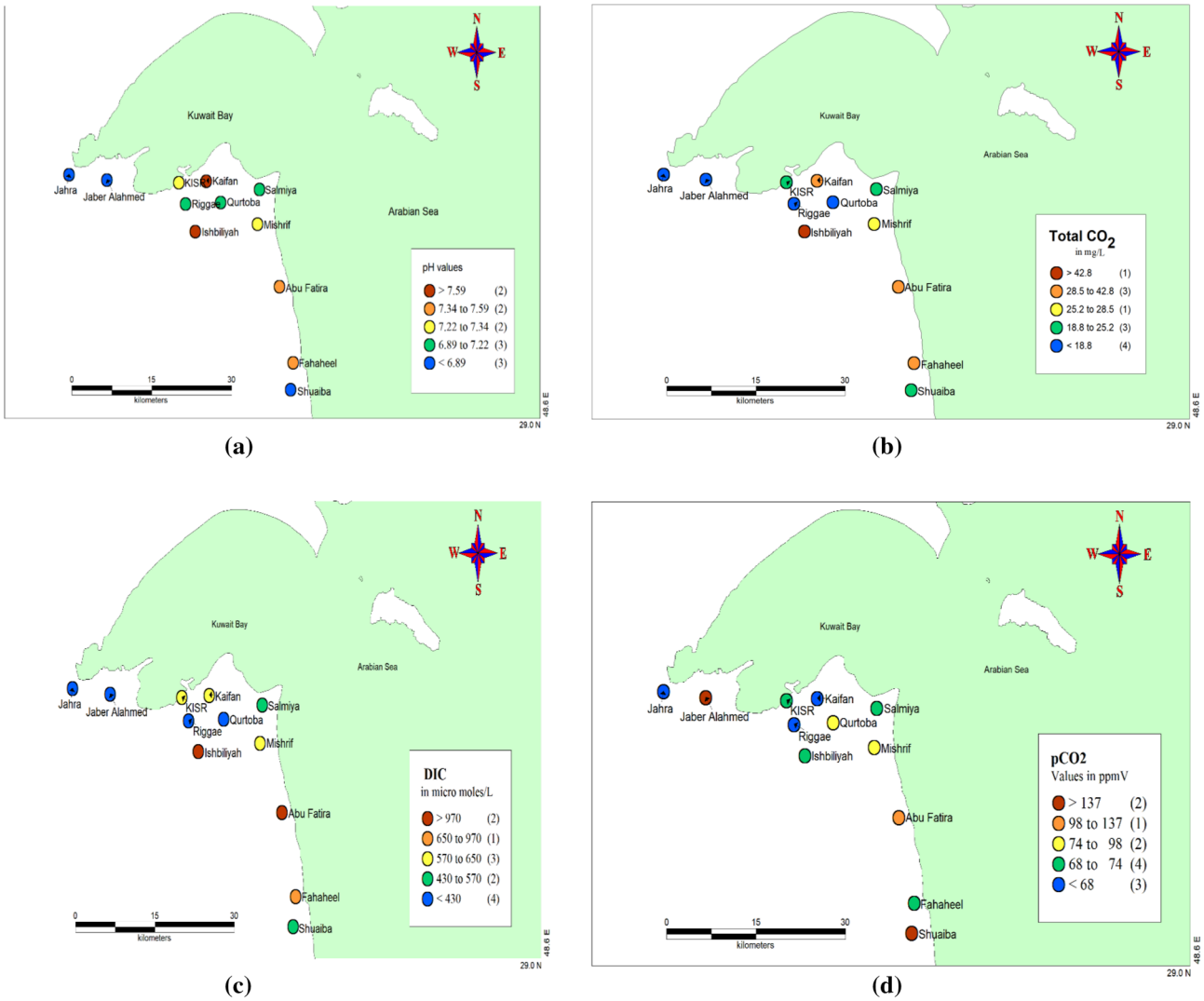


**Fig. 3** **a**, **b**, **c** and **d** Spatial distribution for the average values of pH, Total $CO_2$, DIC and $pCO_2$ in rainwater

## Spatial distribution of pH, total $CO_2$, DIC and $pCO_2$

The mean analytical results pH, total $CO_2$, DIC, and $pCO_2$ of the study areas concerning the residential and industrial region were distributed spatially to understand the areas enriched with $CO_2$ (Fig. 3a–d). Shuaiba, being an industrial region, observed an acidic pH (5.69) with the highest $pCO_2$ (388.73 ppmV). Ishbiliya was reported to contain the highest DIC as 1147.92 µmole/L and total $CO_2$ as 50.41 mg/L due to alkaline pH 7.59. pH above 7.0 usually tends to increase the DIC. Jahra and Riggae areas were noticed with low concentrations of total $CO_2$ (< 10 mg/L). The rainwater samples were categorized into the residential and industrial regions to distinguish the variation in the concentration of total $CO_2$. The output PHREEQC was classified as residential regions and industrial (Table 1) with the pH, alkalinity, and total $CO_2$. In general, uncontaminated rainwater is acidic, but the neutralizing ions present in the atmosphere increase the pH and become alkaline. The chemistry of precipitation waters in Lhasa, Tibet was alkaline with an average of pH 8.36 in 1987–1988 (Zhang et al. 2003). As pH increased, the alkalinity increased, and total $CO_2$ also increased in rainwater samples. The alkalinity of rainwater samples (Table 1) reflect the influence of carbonate dust present in large amounts in

**Table 1** pH, Alkalinity and total $CO_2$ of samples collected during individual rain events from residential and industrial region

| Residential region | | | | | Industrial region | | | | |
|---|---|---|---|---|---|---|---|---|---|
| Sample ID | Date | pH | Alkalinity (mg/L) | Total $CO_2$ (mg/L) | Sample ID | Date | pH | Alkalinity (mg/L) | Total $CO_2$ (mg/L) |
| QR1 | 19.11.2018 | 6.6 | 17.1 | 20 | KS33 | 22.11.2018 | 7.19 | 15.74 | 13.06 |
| QR2 | 22.11.2018 | 7.5 | 13.36 | 10.3 | KS34 | 24.11.2018 | 7.06 | 15.47 | 13.31 |
| QR3 | 24.11.2018 | 6.94 | 28.78 | 26.01 | KS35 | 24.11.2018 | 6.83 | 36.4 | 35.02 |
| QR4 | 28.11.2019 | 6.58 | 16.4 | 20.02 | KS36 | 24.11.2018 | 6.91 | 43.54 | 40.09 |
| QR5 | 13.12.2019 | 7.18 | 16.1 | 13.79 | KS37 | 31.12.2018 | 7.96 | 16.78 | 11.69 |
| QR6 | 16.12.2019 | 7.15 | 20.5 | 17.46 | KS38 | 16.01.2019 | 7.44 | 60.57 | 47.12 |
| QR7 | 16.12.2019 | 7.18 | 11.2 | 9.44 | KS39 | 10.02.2019 | 7.81 | 60.1 | 44.13 |
| QR8 | 17.12.2019 | 7.89 | 28.4 | 21.03 | KS40 | 25.03.2019 | 7.75 | 66.5 | 49.5 |
| QR9 | 17.12.2019 | 6.62 | 26 | 30.69 | KS41 | 27.10.2019 | 7.32 | 54.5 | 42.74 |
| KF10 | 24.11.2018 | 7.67 | 37.94 | 28.5 | KS42 | 27.10.2019 | 7.59 | 55.6 | 42.37 |
| MR11 | 22.11.2018 | 7.46 | 27.63 | 21.51 | KS43 | 16.12.2019 | 6.67 | 6.6 | 7.37 |
| MR12 | 24.11.2018 | 6.98 | 33.81 | 30.06 | KS44 | 16.12.2019 | 6.69 | 9.0 | 9.94 |
| AF13 | 24.11.2018 | 7.34 | 54.07 | 42.79 | KS45 | 16.12.2019 | 7.17 | 22.5 | 18.96 |
| JR14 | 16.11.2018 | 6.3 | 1.1 | 1.8 | KS46 | 16.12.2019 | 7.31 | 7.30 | 5.92 |
| JR15 | 22.11.2018 | 6.71 | 8.85 | 9.39 | KS47 | 16.12.2019 | 7.29 | 19.0 | 15.49 |
| FR16 | 19.11.2018 | 6.78 | 5.82 | 5.93 | KS48 | 16.12.2019 | 7.11 | 16.7 | 14.46 |
| FR17 | 22.11.2018 | 7.23 | 9.62 | 7.91 | KS49 | 16.12.2019 | 7.07 | 19.0 | 16.68 |
| FR18 | 24.11.2018 | 7.16 | 40 | 33.22 | SH50 | 11.02.2019 | 5.69 | 4.74 | 21.41 |
| FR19 | 25.11.2018 | 8.21 | 66.85 | 47.92 | | **Minimum** | **5.69** | **4.74** | **5.92** |
| FR20 | 31.12.2018 | 7.46 | 83.1 | 64.64 | | **Maximum** | **7.96** | **66.5** | **49.5** |
| FR21 | 25.03.2019 | 7.21 | 41.2 | 33.62 | | **Average** | **7.16** | **29.45** | **24.96** |
| JAB22 | 14.11.2018 | 6.76 | 19.67 | 19.87 | | | | | |
| JAB23 | 19.11.2018 | 6.54 | 11.51 | 14.32 | | | | | |
| JAB24 | 24.11.2018 | 6.78 | 17.73 | 17.56 | | | | | |
| RG25 | 19.11.2018 | 6.4 | 5.47 | 7.86 | | | | | |
| RG26 | 22.11.2018 | 6.72 | 8.54 | 9.02 | | | | | |
| RG27 | 24.11.2018 | 7.86 | 73.36 | 5.4 | | | | | |
| RG28 | 24.11.2018 | 7.19 | 4.16 | 3.4 | | | | | |
| SM29 | 22.11.2018 | 6.46 | 3.65 | 4.71 | | | | | |
| SM30 | 24.11.2018 | 7.32 | 45.12 | 35.84 | | | | | |
| IS31 | 10.12.2018 | 7.73 | 78.59 | 58.52 | | | | | |
| IS32 | 16.12.2019 | 7.444 | 54.4 | 42.29 | | | | | |
| | **Minimum** | **6.3** | **1.1** | **1.8** | | | | | |
| | **Maximum** | **8.21** | **83.1** | **64.64** | | | | | |
| | **Average** | **7.1** | **28.44** | **22.34** | | | | | |

Bold indicates Minimum, Maximum, and Average values of whole data

the atmosphere (Kattan 2020), as the acidic nature is generally neutralized by atmospheric dust (Balasubramanian et al. 2001; Al-Momani et al. 2008; Al-Khashman 2009; Rao et al. 2016). The total $CO_2$ in residential region samples was comparatively lower than industrial region samples, but few samples showed higher, especially in the Fahaheel area close to the Industrial sector (Fig. 3b). In general, total $CO_2$ was higher in 2019 compared to 2018 events in the industrial region. This higher trend continued until October 2019, followed by a reduction of total $CO_2$ in December rain events. Dissolved $CO_2$ is the key component governing the pH of rainwater. The rainwater pH is mainly controlled by greenhouse gases (Menz and Seip 2004; Senanayake et al. 2005; Wang and Wang 2006). The change in pH values of rainwater due to the rise in $CO_2$ levels affected the ecosystem, reported by earlier studies (Zhang et al. 2003; Hendershot et al. 1993).

The samples collected on 24 November 2018 in the residential and industrial region were observed to contain high amounts of total $CO_2$ except for two samples from the residential area, Riggae. On observing the total $CO_2$, it was noticed that the residential region of Fahaheel had a maximum concentration (64.6 mg/L) for the sample collected on 31 December 2018. The two samples from Isbhiliya also showed higher values of $CO_2$. The residential samples collected adjacent to the coast had high pH, thus varying the total $CO_2$ concentrations in rainwater. The biological driven carbonate deposition and nutrient loadings to the ocean or surface water bodies also significantly reduce $CO_2$ diffusing from water bodies to the atmosphere (Wang and Wang 2006). An increase in phytoplankton species would increase inorganic carbon into the oceans, contributing to $CO_2$ emissions and results through sea spray (Rousseaux and Gregg 2012). Samples near the coast were neutralized due to the influence of sea spray and the neutralizing ions from anthropogenic dust (Chidambaram et al. 2014). Thus a relatively higher amount of $CO_2$ was noted in the residential regions (Fig. 3b). The contribution of $CO_2$ from the industrial region is mainly due to fuel combustion.

In contrast, in the residential region, $CO_2$ is contributed from automobile exhaust, baking at homes, construction material, and air cooler (Turk et al. 2010; Al-Salem 2015). The direction of wind flow associated with sandstorms enhances the concentration of $CO_2$ (Czikowsky et al. 2018). Other impurities carried into the atmosphere by the effect of wind flow consequently alter rainwater's nature and vary the pH. Thus it is inferred that rainfall acts as the carbon sink by absorption of $CO_2$ (Bharti et al. 2017).

On comparing the average values of pH, alkalinity, and total $CO_2$ concerning time series, it was observed that the alkalinity and total $CO_2$ increased constantly from 2005 to 2019 in both industrial and residential regions whereas pH showed slight variation in the industrial region (Fig. 4). When the total $CO_2$ values were compared with the industrial and residential areas on a temporal basis, residential regions were observed to have higher $CO_2$ than industrial (Fig. 3b). The change in lifestyle and increase in population, and other factors have contributed to more gases in residential regions and increased total $CO_2$, as observed with the rise in pH and alkalinity.

## Dissolved inorganic carbon

The rain events were studied for the variation of DIC in the samples (Fig. 5). There was a drastic increase in the DIC of November–December 2018 events. The samples represented

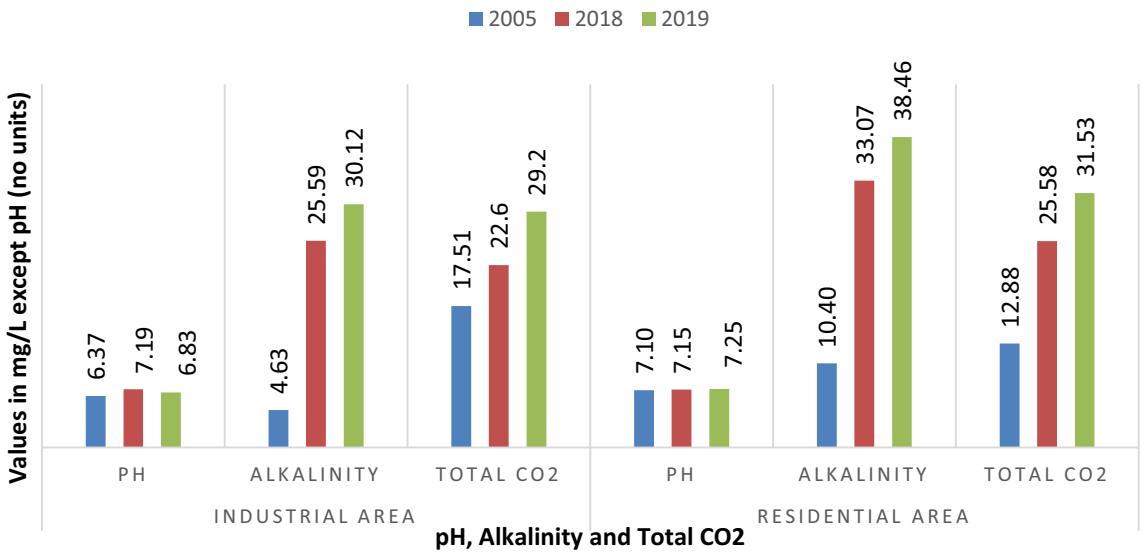


**Fig. 4** Trends of pH, Alkalinity and Total $CO_2$ in rainwater on temporal basis

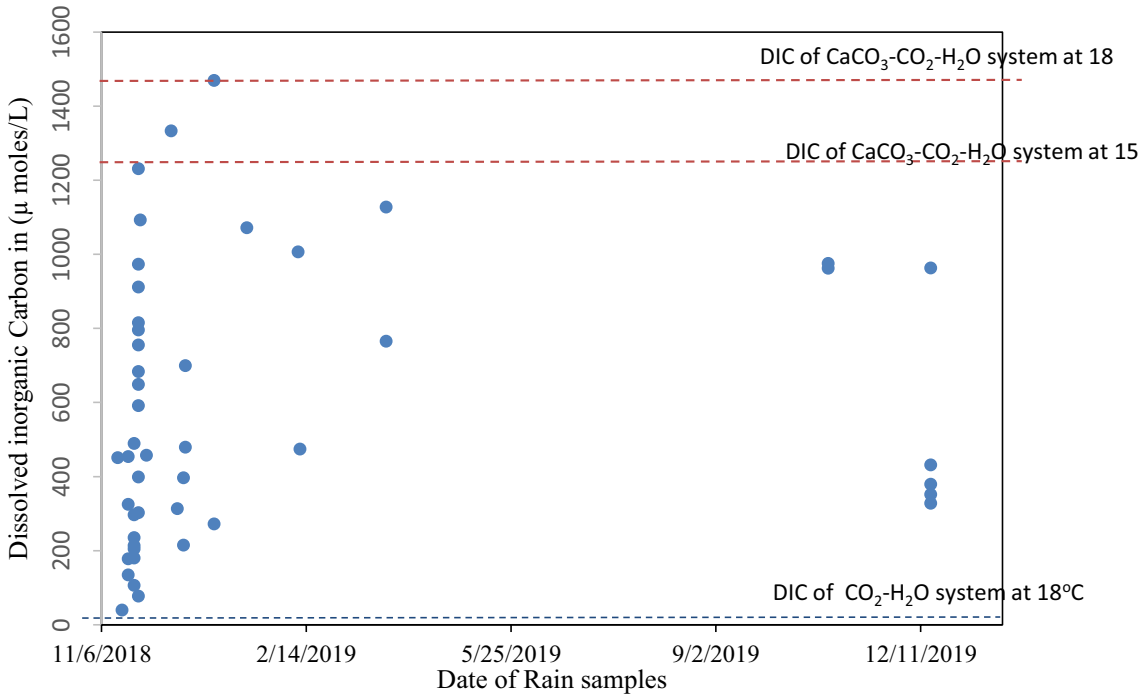


**Fig. 5** DIC of rain events during 2018 and 2019, Comparison of study area with DIC of $CO_2$–$H_2O$ at 18 °C and DIC of $CaCO_3$–$CO_2$–$H_2O$ system at 15 °C and 18 °C (Liu et al. 2010)

different spells on the same day in locations, especially in KISR and Riggae. The values indicated that the first sample collected in the day had a higher value and was subsequently reduced. This phenomenon was also clearly witnessed in the 2019 samples collected at KISR since the first rain event after the summer sandstorm event removed the predominant dust from the atmosphere. In Kuwait, dust storms are more frequent before the seasonal shift from summer to winter (Yassin et al. 2018). The higher values of DIC were observed at KISR located in the southern boundary of Kuwait Bay, and a few samples of Farwaniya, Ishbiliya, and Salmiya represented the western region of the study area (Fig. 3c). Atmospheric dust primarily from the inland desert influenced the DIC in the rain shower of the region. Other factors that influence the natural $CO_2$ dissolution in rainwater are wind speed and direction, the atmospheric temperature during the rain event, and the sandstorms prior to the event. So, the interplay of these events during 24 November 2018, 10 and 30 December 2018 has increased DIC concentration (Fig. 5) in rainwater.

Studies have indicated that high wind speed, usually greater than 20 m/s and precipitation above 15 mm, scavenges the $CO_2$ (Pathakoti et al. 2018). In contrast, in the study region, the wind speed was less than 20 m/s and precipitation was noticed in a few rain events with less than 10 mm. So the wind speed and rainfall amount have contributed to higher $CO_2$. The rain events show that SSE and ESE direction of the wind with speed ranging from 3.9 to 4.4 m/s was predominant during 14–16 November 2019. Subsequently, from 22 to 24 November 2018 the prevailing direction was from SSE and NW with an average wind speed of 6.7–7.5 m/s, but the rain events during 10 and 21 December 2019 were from NE and had an average speed of 1.1 m/s. The lesser wind speed has facilitated the reaction time of the dust with the rain droplets, thereby increasing the DIC concentration in rainwater during this period. In general, the value of DIC is greater than 800 µmoles/L were noted in western parts of the study area and the South of Kuwait Bay.

It is calculated that 380ppmV is the global mean atmospheric $CO_2$ (GMAP) at global mean annual surface temperature (GMAST) 15 °C has 20 µmoles/L of DIC in $CO_2$ -$H_2O$ system (Dreybrodt 2012) at equilibrium. There are two probable reactions of Ca with $CO_2$, either as ($CaCO_3$–$CO_2$–$H_2O$) or with Ca– silicate. In carbonate system, the dissolution of $CaCO_3$ consumes less $CO_2$, as one $CO_2$ is dissolved for each Ca to form two $HCO_3^-$. In this system at equilibrium condition, the DIC is estimated to be 1231 µmoles/L at GMAP and GMAST, which is 66 times greater than the DIC of the $CO_2$-$H_2O$ system. In the silicate system, weathering of the silicate minerals also consumes relatively more $CO_2$ (Dupré et al. 2003; Mortatti and Probst 2003). The reactions of the Ca-carbonate and Ca-silicate system with $CO_2$–$H_2O$ can be expressed as follows (Li et al. 2013, 2016).

$$H_2O + CO_2 + CaCO_3 \rightleftharpoons 2HCO_3^- + Ca^{2+}. \quad (3)$$

$$3H_2O + 2CO_2 + 2CaSiO_4 \rightleftharpoons 2HCO_3^- + H_4SiO_4 + Ca^{2+}. \quad (4)$$

It is clear from the above reactions that half of the $HCO_3^-$ in the carbonate system and total $HCO_3^-$ in the silicate system is derived from the atmospheric $CO_2$. Thus, atmospheric sequestration is mainly influenced by the above processes. The silicate minerals are generally reported to have a slow weathering rate and very slow solubility compared to carbonates (Singh et al. 2005; Wu et al. 2005, 2008; Moon et al. 2007). The contribution of $CO_2$ to the atmospheric sink is less significant due to silicate weathering because of low reaction kinetics. But the carbonate system is very dynamic and plays a key role in the $pCO_2$ and DIC of rainwater. In Kuwait, the carbonate dissolution is facilitated in rainwater chiefly by the carbonate dust attributed to the dolomitic formations.

The rainwater DIC flux was determined as the product of the mean DIC and total rainwater (Shiklomanov 1993; Arsene et al. 2007; Ladouche et al. 2009; Celle-Jeanton et al. 2009). The total annual rainfall during 2018 and 2019 was reported as 343.8 mm and 69.3 mm, respectively. Therefore, the average DIC derived from rainwater in 2018 and 2019 was 540 µmoles/L and 568 µmoles/L, respectively. Hence, the rainwater flux during these years was estimated to be 1,85,652 µmoles/L and 39,362 µmoles/L during the years 2018 and 2019.

## Comparison of DIC with $pCO_2$

The DIC was compared to the $pCO_2$ in rainwater to determine the influence of carbonate dust. The samples of 2018 and 2019 were compared to the equilibrium values of $pCO_2$ of $CO_2$–$H_2O$ (Longinelli et al. 2005; IPCC 2013) equilibrium values of $CO_2$ for $CaCO_3$–$CO_2$–$H_2O$ system and the projected global mean value at 18 °C along with the observed values during 2005. There was excess rain shower during 2018 than normal years. The $pCO_2$ value ranges from 6.78 to 227.9 ppmV during 2018, while 14.02 to 388 ppmV in 2019 (Fig. 6). Similarly, DIC varies from 39.7 to 1469.6 µmoles/L in 2018 and 134.7–1127.46 µmoles/L during 2019. The samples of 2018 had a wide range of DIC compared to 2019, greater than equilibrium values of the $CO_2$-$H_2O$ system but less than $CaCO_3$–$CO_2$–$H_2O$ at 18 °C. The global mean DIC in rainwater is 82.8 µmoles/L, which is significantly lesser than the equilibrium value of 1231 µmoles/L, due to the short interaction time of rainwater with the carbonate dust $< 10^4$ s (Dreybrodt 2012). They do not attain equilibrium instantly and are believed to have a value lesser than the equilibrium value. The DIC value also changes with atmospheric temperature. A definite trend was observed between $pCO_2$ and DIC except for positive linearity at equilibrium condition of $CO_2$–$H_2O$ and $CaCO_3$–$CO_2$–$H_2O$ system. A wide range of $pCO_2$ was observed in 2019 samples than the 2018 and 2005 samples. All the samples except one are below the equilibrium value of $pCO_2$ reported at different temperatures for both the $CO_2$–$H_2O$ system as well as $CaCO_3$–$CO_2$–$H_2O$. The above equilibrium values may be because several organic carbon species like polycarboxylic acid substances are surface-active and form nuclei for

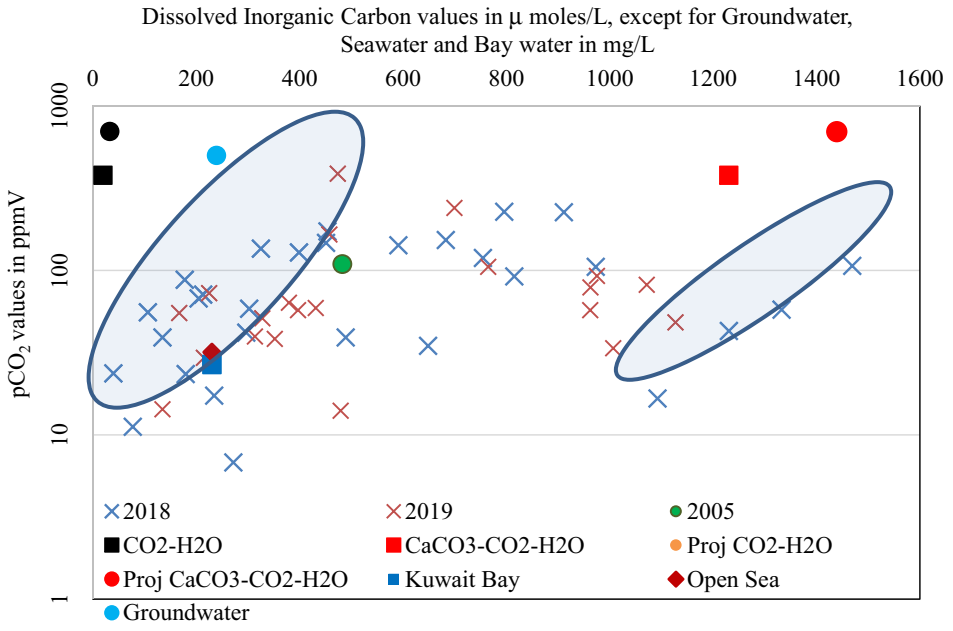


**Fig. 6** Comparison of $pCO_2$ study area with Equilibrium value of $CO_2$–$H_2O$ and $CaCO_3$–$CO_2$–$H_2O$, Global projected $CO_2$–$H_2O$ and $CaCO_3$–$CO_2$–$H_2O$ (Liu et al. 2010), Open Sea (Bhandary et al. 2018, Kuwait Bay (Ali and Chidambaram 2020) and Groundwater (Sabarathinam et al. 2020a, b)

condensation (Orlović-Leko et al. 2010). Further, Shulman et al. (1996) inferred that these compounds facilitate nucleation by decreasing the supersaturation level, the surface tension and hygroscopicity of the inorganic suspension in air mass (Saxena et al. 1995), which also influences the association of major ions to $CO_2$ in rainwater and thus the $pCO_2$ values.

## DIC and $pCO_2$ comparison of rainwater with groundwater

The DIC in the Kuwait aquifers were compared with the DIC of rainwater samples of the current study (Fig. 6). The average DIC value was derived from the analytical results of the groundwater samples collected for previous studies in the region (Sabarathinam et al. 2020b). The groundwater of the region is mostly saline, and the DIC concentration is on an average of 239 mg/L, with a $pCO_2$ value of 501 ppmV. The lithology of the older Dammam aquifer in Kuwait is mainly dolomitic and that upper Kuwait group aquifer is predominantly arenaceous, with intercalations of Chert and Gypsum (Mukhopadhyay et al. 1996). The behaviours of the Karst aquifer and their associated pH were studied in different parts of the world (Liu et al. 2007; Macpherson et al. 2008). The $pCO_2$ relationship to pH in the coastal groundwater (Rajendiran et al. 2019), continental silicate aquifers (Panda et al. 2019), and the alluvial aquifers (Chidambaram et al. 2011) proved that a negative association exists between the two variables. The reforestation and temperatures are some of the significant factors reported to increase the soil $pCO_2$ (Liu and Zhao 2000). This phenomenon was reflected with the increased $HCO_3^-$ value in groundwater during summer. The high $pCO_2$ favours the dissolution of carbonates and thus enhances the $HCO_3^-$ values in groundwater, but the groundwaters of both the aquifers in Kuwait are saline, and the predominant ions are $Na^+$ and $Cl^-$ (Chidambaram et al. 2020). The $CO_2$ generated from the soil facilitates the dissolution of dolomite and calcite in the Karstic aquifer (Macpherson et al. 2008). The increase of $CO_2$ in groundwater indicates that this component of the hydrological cycle is an excellent sink for $CO_2$ through the dissolution of carbonate rocks. The saturation state of calcite is observed to be near zero in Dammam aquifers and much negative in non-carbonate Kuwait group aquifer (Sabarathinam et al. 2020a). Similar results were observed globally (Millot et al. 2003; Liu et al. 2010; Devaraj et al. 2018). The greater volume of groundwater and lesser possibility of return flux (except in the discharge region) serve as an excellent carbon store compared to atmospheric $CO_2$ sink and the surface water bodies (Kempe 1979). Since $CO_2$ production in soil increases with temperature, the release of $CO_2$ from the soil matrix is significantly reduced due to the complete or partial saturation of the pore spaces. Such variations are also dependent on the frequency and duration of rain event (Kabwe et al. 2006).

## DIC and $pCO_2$ of the Bay and open Seawater

The earlier studies on sea-air $CO_2$ flux exchange have not considered the $CO_2$ transfer from hot deposition from the atmosphere and the chemical dilution at the surface due to rainfall (Ishii et al. 2004; Feely et al. 2006). The surface water bodies act as biological pumps as oceans exhibit huge reservoirs for the atmospheric $CO_2$ by the uptake of DIC during photosynthesis of the oceanic biota (Cassar et al. 2004; Blain et al. 2007). The ratio between the carbons emitted to the atmosphere to that of sediment buried showed a relationship of 0.08, indicating the eutrophic lake's effectiveness as a carbon sink (Yang et al. 2008). Further high $pCO_2$ has increased and calcified the productivity of Emiliania Huxleyi, indicating their response and adaptation to high $pCO_2$ waters. The standard mechanism of $pCO_2$ is generally observed at a depth of 3.5 m below the sea surface, and the role of this interface, the top ocean layer on $pCO_2$, is not considered in climate models. This phenomenon is very significant in ocean regions represented by high rainfall and low wind. The $pCO_2$ at the ocean-atmospheric interface is also altered by the variation in sea skin temperature (Ashton et al. 2016) apart from the turbulence during a rain event (Ho et al. 2004; Zappa et al. 2009). The data on $CO_2$ variations along with the interface during short, intense rain events are scarce.

The DIC and the $pCO_2$ values of the Kuwait Seawater and the Bay water were derived from the results of the previous studies in the region (Bhandary et al. 2018; Ali and Chidambaram 2020). Though there is no significant variation in DIC concentration, the $pCO_2$ of the seawater is relatively higher than the samples representing Kuwait Bay (Fig. 6). This is because the surface dwellers, especially plankton and organism with carbonate shells, remove atmospheric $CO_2$. Subsequently, these dead species, along with their faecal material, settle into the ocean floor. This process facilitates the reduction of $pCO_2$ at the ocean surface. It enhances the $pCO_2$ uptake capacity from the atmosphere and the newly derived DIC from rainwater and surface water sources. The rate of movement of water in the Bay is relatively lesser than the open sea (Pokavanich and Alosairi 2014). This variation in the residence time, current and tidal movement moderates the physical conditions of the Bay and open sea environment leading to the variation in $pCO_2$ values. Further, a sizeable quantum of the organic domestic sewage is discharged into the Bay (Sabarathinam et al. 2019), influencing the $pCO_2$ values of the Bay and the open sea. The precipitation of $CaCO_3$ resulted in the production of $CO_2$ counteracted by the stored and produced organic carbon in the surface of water

bodies (Lerman and Mackenzie 2005), and the relationship is explained as follows.

$$H_2O + CO_2 + CaCO_3 \rightleftharpoons Ca^{2+} + 2HCO_3^-. \quad (5)$$

Fertilization reduces the $pCO_2$ in these regions and enhances the $CO_2$ in the atmosphere (Ternon et al. 2000). The return of $CO_2$ into the atmosphere through biotic respiration also plays a key role in $CO_2$ dynamics (Cole et al. 2007; Zondervan 2007). In the $CaCO_3$ predominant system, dissolved by acidic rainwater ($H_2CO_3$), there is an expected release of $CO_2$ back to the atmosphere.

$$CaCO_3 + H_2CO_3 \rightleftharpoons Ca(OH)_2 + 2CO_2. \quad (6)$$

$CO_2$ is released into the atmosphere during continental weathering through carbonate precipitation on the ocean floor. In addition, the enhanced $CO_2$ uptake by the photosynthetic process also plays a key role in oceanic CO2, as the planktonic species growth is prominent in Kuwait's open sea environment (Devlin et al. 2019).

The spatial extent of the fresh rainwater on the surface layer governs the $pCO_2$ at the air–water interface. The dilution effect observed along the sea surface reduces the $pCO_2$ along the boundary, and this effect is sustained for a significant period when there is low wind and heavy rainfall (Henocq et al. 2010). Still, the freshwater due to rain can be spread to a larger area through surface currents. In Kuwait, the earlier studies (Pokavanich and Alosairi 2014) indicate that the residence time and the relative water movement is less than other regions globally due to the density influenced by salinity, especially in the Bay (Sabarathinam et al. 2019).

## Projection of total $CO_2$ against the ratio of ($HCO_3^-$/ $Ca^{2+} + Mg^{2+}$)

Total $CO_2$ in rainwater samples were projected against the ratio of ($HCO_3^-$/ $Ca^{2+} + Mg^{2+}$). $Ca^{2+}$ and $Mg^{2+}$ are the common neutralizing ions present in rainwater due to the carbonate dust in the atmosphere. The concentration of $HCO_3^-$ varies dissolution of the dust depending on the reaction time with the rainwater and the pH. The pH is also governed by the neutralizing ions present in the rainwater, similar to the study in groundwater containing dominant ions of $Ca^{2+}$ and $Mg^{2+}$ (Li et al. 2013, 2019). Hence, the $HCO_3^-$/( $Ca^{2+} + Mg^{2+}$) ratio will provide a relative variation trend of $Ca^{2+} + Mg^{2+}$and the influence of carbonate dust in rainwater. The average values of the samples in the study area were compared to global values and that of the GCC region. The average total $CO_2$ value of 5 mg/L, with an average ratio of 1.70 of $HCO_3^-$ and ($Ca^{2+} + Mg^{2+}$), was observed in the Indian rainwater samples (Fig. 7). The Indian southwest monsoon showers reflected alkaline nature on long-term observation. The linear relation between $HCO_3^-$ and ($Ca^{2+} + Mg^{2+}$) in Indian rainwater samples indicated carbonate dust as a crustal source, which tends to neutralize the $H^+$ ions present in rainwater (Rastogi and Sarin 2005).

On the contrary acidic pH was observed in the southern coastal region of India during the southwest monsoon season due to the minor influence of Na, and Cl ions due to sea spray, in the coastal rain showers (Chidambaram et al. 2014). The $HCO_3^-$/($Ca^{2+} + Mg^{2+}$) ratio of samples from USA, Spain and Brazil were within a range of 0.2 to 0.1 values (Fig. 6). The acidity of precipitation in the United States was

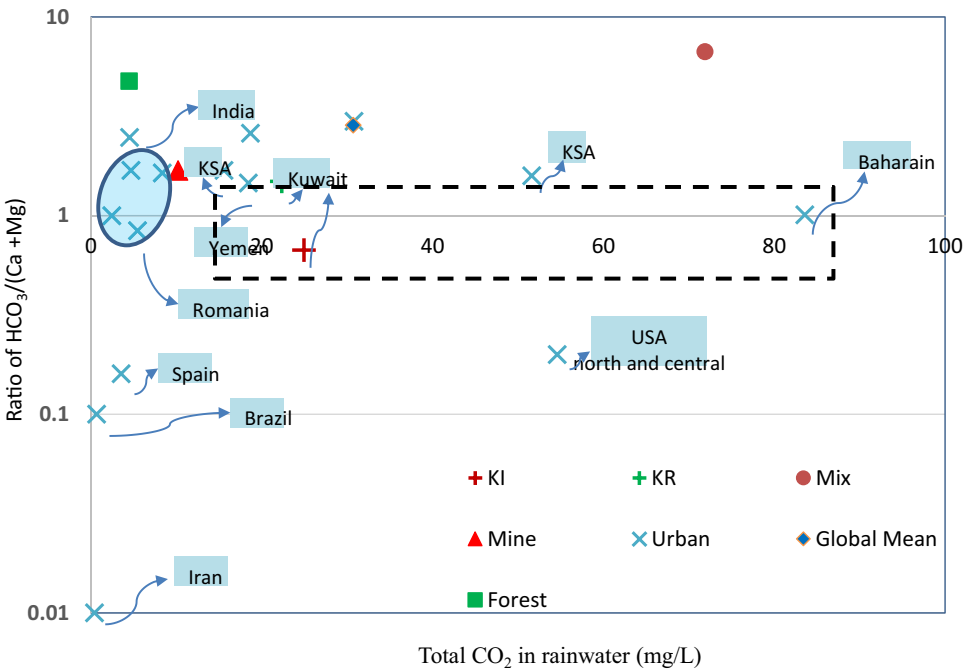


**Fig. 7** Influence of the carbonate dust on the total $CO_2$ in rainwater, a comparison of the Kuwait rainwater ratio to global values(calculated as average from all areas) and to those representing different land use patterns such as Baharin (Naik et al. 2017), Brazil (Facchini Cerqueira et al. 2014), Iran (Naimabadi et al. 2018), King of Saudi Arabia (KSA) (Ahmed et al. 1990), (Alabdula'aly and Khan 2000), Spain (Moreda-Piñeiro et al. 2014), Yemen (Saleh et al. 2017), North and Central USA, Romania, India, Mix, Mining, Forest (Liu et al. 2010)

reported to be changed due to $NH_3$ and alkaline soil dust in the atmosphere, which tend to neutralize the anthropogenically derived acids (Munger 1982). Similar observations on the variation of acidity of rainfall in Brazil showed that sugarcane burning, soil dust and industrial emissions are the main sources that control the acidity of rainwater (Lara et al. 2001). The studies on precipitation in Tibet indicated that alkalinity prevailed in the samples though $pCO_2$ decreases with an increase in elevation, attributed to the presence of $CaCO_3$ rich dust in the atmosphere (Zhang et al. 2003).

The sample of Iran had the least ratio of 0.01, with the lowest total $CO_2$ concentration of 0.42 mg/L. The average values of total $CO_2$ in the samples of Kuwait ranged from 20 to 30 mg/L and the ratio of $HCO_3^-/(Ca^{2+}+Mg^{2+})$ was higher in the residential regions than the industrial regions. The studies related to $CO_2$ emissions in the urban region of Japan observed higher values in areas using reclaimed water (Shimizu et al. 2013). It leads to the fact that the average sample values from GCC (Kingdom of Saudi Arabia, Bahrain and Yemen) have total $CO_2$ values ranging from > 15 mg/L to less than 90 mg/L and the ratio of $HCO_3^-/(Ca^{2+}+Mg^{2+})$ fall predominantly between 1 and 2. Thus, a distinct signature of the samples representing the Arabian Peninsula region was observed. Further, the average values of samples of the present study were well below the global mean value of total $CO_2$ and $HCO_3^-/(Ca^{2+}+Mg^{2+})$ in the rainwater samples. The sample representing a mixed land use pattern had the higher value of both the variables (Fig. 6).

The coastal rainwater is also affected by the concentration of $Na^+$ and $Cl^-$ due to the sea spray effect (Chidambaram et al. 2014). The increase of these ions also alters the total ionic concentration of rainwater. The $CO_2$ content is influenced predominantly by carbonate dust than the sea spray process. The impact of sea spray is observed only in the regions with a predominant sea breeze. Hence, it is inferred that $Ca^{2+}$ and $Mg^{2+}$ ions play a significant role in neutralization than $Na^+$ and $Cl^-$. The rainwater compositions reported in the peninsular region show a characteristic zone of representation in the plot indicating the ratio range between 1 and 2 and the total $CO_2$ between 15 and 90 mg/L.

## Correlation analysis

### Spearman correlation

Spearman correlation analysis was adopted to study the correlation between major ions and total $CO_2$ in rainwater of residential and industrial regions using SPSS 2.0 software. The output data (Table 2) from the residential region exhibited that pH was strongly associated with EC, Alkalinity, ions such as $Na^+$, $Ca^{2+}$, $F^-$, $NO_3^-$, and $SO_4^{2-}$ and weakly correlated with $Mg^{2+}$ and total $CO_2$. Likewise, EC and TDS were correlated to alkalinity, ions such as $Na^+$, $K^+$, $Ca^{2+}$, $Mg^{2+}$, and major anions $F^-$, $Cl^-$, $NO_3^-$ and $SO_4^{2}$. Alkalinity was strongly correlated to total $CO_2$ and ions $Na^+$, $Ca^{2+}$, $Mg^{2+}$, $NO_3^-$ and $SO_4^{2}$- but weekly associated with $F^-$ and $Cl^-$. Alkaline soil dust eroded to the atmosphere due to wind, and a few gases neutralizing the anthropogenic acidic concentrations increases the pH and the dissolution of $CO_2$ (Munger, 1982). $Na^+$ is dependent on $K^+$, $Ca^{2+}$, $Mg^{2+}$, $F^-$, $Cl^-$, $Br^-$, $NO_3^-$ and $SO_4^{2}$. A significant observation from the Spearman correlation result was total $CO_2$ is strongly associated with pH, EC, Alkalinity, $Na^+$, $K^+$, $Ca^{2+}$, $Mg^{2+}$, $NO_3^-$, but weekly correlated to $F^-$, $Cl^-$ and $SO_4^{2-}$. Also, it was observed that $NH_4^+$ was negatively associated with temperature. It means pH, ions, and alkalinity are the major influencing factors for the dissolution of $CO_2$. The cations associated with the bicarbonates are mainly from the soil eroded in dust form that contributes to $CO_2$ (Cerqueira et al. 2014). The industrial region exhibited a similar relation to samples from the residential region, but significant positive correlations (Table 2a, b) was observed between temperature, total $CO_2$ and negative correlation with $PO_4^{3-}$.

### Principal component analysis (PCA)

The PCA was also applied to evaluate the relationships between the analytes present in the rainwater (Wu et al. 2014, 2020; Li et al. 2019; Ren et al. 2021). The factor analysis adopting varimax rotation (Table 3) resulted in six residential and four industrial regions with an eigenvalue greater than 1. The first factor accounted for approximately 43.0% of the variance, reflecting a strong positive association of total $CO_2$ with EC, alkalinity, and major ions. It indicates that the ions and bicarbonates are purely from crustal sources. The crustal source of dust in Kuwait is the primary source of contamination in rainwater (Samayamanthula et al. 2021). The abundances of ions and alkaline nature in precipitation of semi-arid region, India suggested that the ions are mostly crustal and eroded as soil dust (Cerqueira et al. 2014). The second major factor loadings contribute to approximately 12.2% of the variance with a strong association between pH, alkalinity, and total $CO_2$. This factor depicts clearly that as pH increases, alkalinity increases and simultaneously influences the total $CO_2$. The bicarbonates are strongly associated with $Mg^{2+}$and $K^+$ which neutralizes the acid originated from dust (Rastogi and Sarin 2005; Cerqueira et al. 2014). Only 10% contributes from the third factor with an impact of ammonium and nitrite ions. Temperature influence on the rainwater was observed from the fourth factor with 9.8%. There is no representation of ions or pH, temperature, EC in the fifth factor. Bromide and phosphate ions were associated with the sixth factor with a contribution of 7.3%.

**Table 2** **a** Spearman correlations of rainwater chemistry and total $CO_2$ of residential region

| | | Temperature | pH | EC | Alkalinity | $Na^+$ | $NH_4^+$ | $K^+$ | $Ca^{2+}$ | $Mg^{2+}$ | $F^-$ | $Cl^-$ | $NO_2^-$ | $Br^-$ | $NO_3^-$ | $PO_4^{3-}$ | $SO_4^{2-}$ | Total $CO_2$ |
|---|---|---|---|---|---|---|---|---|---|---|---|---|---|---|---|---|---|---|
| Temperature | CC-Res | 1.00 | 0.18 | 0.24 | 0.26 | 0.30 | − 0.37 | 0.12 | 0.42* | 0.02 | 0.41* | 0.48** | 0.44* | 0.19 | 0.23 | 0.06 | 0.38* | 0.11 |
| pH | | | 1.00 | 0.56** | 0.69** | 0.44* | 0.36* | 0.25 | 0.62** | 0.36* | 0.56** | 0.24 | − 0.02 | 0.06 | 0.51** | 0.15 | 0.49** | 0.47** |
| EC | | | | 1.00 | 0.85** | 0.73** | 0.20 | 0.46** | 0.77** | 0.89** | 0.48** | 0.63** | 0.12 | 0.19 | 0.72** | 0.31 | 0.73** | 0.80** |
| Alkalinity | | | | | 1.00 | 0.53** | 0.24 | 0.28 | 0.77** | 0.69** | 0.43* | 0.40* | 0.00 | 0.11 | 0.56** | 0.28 | 0.51** | 0.86** |
| Na + | | | | | | 1.00 | 0.09 | 0.73** | 0.73** | 0.72** | 0.68** | 0.80** | 0.14 | 0.31 | 0.81** | 0.24 | 0.80** | 0.55** |
| $NH_4^+$ | | | | | | | 1.00 | 0.01 | − 0.03 | 0.20 | − 0.04 | − 0.08 | 0.09 | 0.00 | 0.47** | − 0.05 | 0.00 | 0.12 |
| $K^+$ | | | | | | | | 1.00 | 0.52** | 0.54** | 0.48** | 0.62** | 0.15 | 0.20 | 0.51** | 0.38* | 0.64** | 0.33 |
| $Ca^{2+}$ | | | | | | | | | 1.00 | 0.66** | 0.67** | 0.70** | 0.12 | 0.21 | 0.63** | 0.26 | 0.82** | 0.66** |
| $Mg^{2+}$ | | | | | | | | | | 1.00 | 0.36* | 0.66** | 0.14 | 0.10 | 0.63** | 0.36* | 0.68** | 0.72** |
| $F^-$ | | | | | | | | | | | 1.00 | 0.48** | 0.24 | 0.10 | 0.54** | − 0.09 | 0.74** | 0.35 |
| $Cl^-$ | | | | | | | | | | | | 1.00 | 0.30 | 0.23 | 0.65** | 0.23 | 0.82** | 0.38* |
| $NO_2^-$ | | | | | | | | | | | | | 1.00 | 0.04 | 0.32 | 0.02 | 0.25 | − 0.01 |
| $Br^-$ | | | | | | | | | | | | | | 1.00 | 0.23 | 0.31 | 0.25 | 0.02 |
| $NO_3^-$ | | | | | | | | | | | | | | | 1.00 | 0.12 | 0.68** | 0.56** |
| $PO_4^{3-}$ | | | | | | | | | | | | | | | | 1.00 | 0.21 | 0.29 |
| $SO_4^{2-}$ | | | | | | | | | | | | | | | | | 1.00 | 0.43* |
| Total $CO_2$ | | | | | | | | | | | | | | | | | | 1.00 |

b Spearman correlations of rainwater chemistry and total $CO_2$ of industrial region

| | | Temperature | pH | EC | Alkalinity | $Na^+$ | $NH_4^+$ | $K^+$ | $Ca^{2+}$ | $Mg^{2+}$ | $F^-$ | $Cl^-$ | $NO_2^-$ | $Br^-$ | $NO_3^-$ | $PO_4^{3-}$ | $SO_4^{2-}$ | Total $CO_2$ |
|---|---|---|---|---|---|---|---|---|---|---|---|---|---|---|---|---|---|---|
| Temperature | CC-Ind d | 1.00 | 0.04 | 0.34 | 0.44 | 0.32 | − 0.42 | 0.14 | 0.52* | 0.18 | 0.40 | 0.14 | 0.45 | 0.07 | 0.36 | − 0.04 | 0.30 | 0.54* |
| pH | | | 1.00 | 0.62** | 0.63** | 0.53* | 0.38 | 0.45 | 0.62** | 0.65** | 0.23 | 0.53* | 0.04 | 0.43 | 0.40 | 0.23 | 0.43 | 0.38 |
| EC | | | | 1.00 | 0.74** | 0.90** | 0.45 | 0.75** | 0.96** | 0.95** | 0.65** | 0.87** | 0.28 | 0.60** | 0.88** | 0.29 | 0.91** | 0.61** |
| Alkalinity | | | | | 1.00 | 0.68** | 0.14 | 0.64** | 0.83** | 0.77** | 0.27 | 0.65** | 0.19 | 0.30 | 0.54* | − 0.04 | 0.49* | 0.87** |
| Na+ | | | | | | 1.00 | 0.42 | 0.66** | 0.86** | 0.89** | 0.66** | 0.96** | 0.23 | 0.66** | 0.85** | 0.50* | 0.83** | 0.72** |
| $NH_4^+$ | | | | | | | 1.00 | 0.64** | 0.33 | 0.45 | 0.18 | 0.53* | − 0.11 | 0.47 | 0.56* | 0.45 | 0.54* | 0.09 |
| $K^+$ | | | | | | | | 1.00 | 0.72** | 0.78** | 0.34 | 0.72** | 0.12 | 0.42 | 0.73** | 0.24 | 0.65** | 0.56* |
| $Ca^{2+}$ | | | | | | | | | 1.00 | 0.87** | 0.65** | 0.79** | 0.35 | 0.51* | 0.86** | 0.26 | 0.84** | 0.72** |
| $Mg^{2+}$ | | | | | | | | | | 1.00 | 0.53* | 0.90** | 0.22 | 0.59* | 0.78** | 0.23 | 0.80** | 0.63** |
| $F^-$ | | | | | | | | | | | 1.00 | 0.55* | 0.56* | 0.30 | 0.73** | 0.53* | 0.71** | 0.32 |
| $Cl^-$ | | | | | | | | | | | | 1.00 | 0.10 | 0.72** | 0.8** | 0.5* | 0.79** | 0.68** |
| $NO_2^-$ | | | | | | | | | | | | | 1.00 | − 0.08 | 0.45 | 0.09 | 0.37 | 0.21 |
| $Br^-$ | | | | | | | | | | | | | | 1.00 | 0.48* | 0.53* | 0.57* | 0.35 |
| $NO_3^-$ | | | | | | | | | | | | | | | 1.00 | 0.44 | 0.94** | 0.53* |
| $PO_4^{3-}$ | | | | | | | | | | | | | | | | 1.000 | 0.38 | 0.170 |
| $SO_4^{2-}$ | | | | | | | | | | | | | | | | | 1.000 | 0.46 |
| Total $CO_2$ | | | | | | | | | | | | | | | | | | 1.00 |

**Correlation is significant at the 0.01 level (2-tailed)

*Correlation is significant at the 0.05 level (2-tailed)

In the industrial region (Table 3), the first factor loadings show 52.2% of the variance with an association between EC, TDS, alkalinity, ions and total $CO_2$, temperature, and nitrite. According to the second-factor loadings, temperature influenced nitrite and weakly correlated with $Mg^{2+}$ with 13.9% variance. The third factor indicates that temperature and total $CO_2$ are negatively associated with $PO_4^{3-}$ with 11.7% variance. Finally, pH was correlated to $Mg^{2+}$ with a variance of 10.7% according to the fourth-factor loadings. The report of IPCC (2013) states that the increase of $CO_2$ in the atmosphere results in increased soil and air temperature. On the other hand, the elevated temperature enhances soil respiration leading to the addition of $CO_2$ to the atmospheric stock.

The residential and industrial regions of PCA reflected that the dissolution of ions occurs from the same source in both regions. Additionally, the industrial region was governed by wind speed and direction. Hence, it is clear that pH influences the dissolution of $CO_2$. It should also be noted that the biogenic emission and the fossil-derived carbon contributes to the organic carbon stock in the atmosphere (Tsigaridis and Kanakidou 2003; Spracklen et al. 2008; De Gouw and Jimenez 2009). Predominantly the primary organic carbon is converted to secondary organic aerosols in the atmosphere (Hallquist et al. 2009). Organic carbon removal from the atmosphere through precipitation also plays a significant role in carbon flux transfer (Iavorivska et al. 2016). The marine region had lesser organic carbon values than that of the continental precipitation, and it varied with the distance from the coast. The volatile organic gases in air and water are expected to vary by chemical reactions (Ervens et al. 2011). The chemistry of rainwater is chiefly governed by natural than anthropogenic sources (Liu et al. 2010). It is also mainly due to the prevalence of $CaCO_3$ dust in that atmosphere, either calcite or dolomite dust. But the predominant extreme acidic rain events in the industrial regions are mainly in the downwind direction.

## Conclusions

The study has derived the following conclusions:

1. Rainwater representing both residential and industrial regions acts as a sink for atmospheric $CO_2$.

**Table 3** Rotated Component Matrix[a] of rainwater chemistry and total $CO_2$ of residential and industrial Regions in Kuwait

| | Residential Region of Kuwait | | | | | | Industrial Region of Kuwait | | | |
|---|---|---|---|---|---|---|---|---|---|---|
| Parameter | R-1 | R-4 | R-3 | R-4 | R-5 | R-6 | I-1 | I-2 | I-3 | I-4 |
| Temperature | 0.00 | 0.19 | − 0.14 | 0.90 | 0.01 | 0.15 | 0.06 | 0.52 | 0.56 | − 0.37 |
| pH | 0.25 | 0.73 | − 0.06 | 0.00 | − 0.59 | 0.09 | 0.20 | 0.10 | 0.38 | 0.85 |
| EC | 0.86 | 0.48 | 0.03 | 0.00 | 0.10 | 0.01 | 0.99 | 0.03 | 0.13 | 0.05 |
| Alkalinity | 0.57 | 0.77 | 0.00 | 0.10 | 0.02 | 0.08 | 0.46 | 0.32 | 0.77 | 0.17 |
| Na + | 0.93 | 0.21 | 0.02 | 0.08 | 0.03 | − 0.02 | 0.98 | − 0.01 | 0.11 | 0.06 |
| NH4 + | 0.05 | 0.05 | 0.90 | − 0.36 | 0.06 | − 0.02 | 0.87 | − 0.18 | − 0.23 | 0.01 |
| K + | 0.89 | 0.01 | − 0.18 | − 0.12 | 0.09 | 0.36 | 0.91 | − 0.01 | 0.19 | 0.07 |
| Ca2 + | 0.86 | 0.24 | − 0.03 | 0.19 | − 0.23 | 0.04 | 0.98 | 0.08 | 0.15 | 0.04 |
| Mg2 + | 0.90 | 0.32 | 0.03 | − 0.10 | 0.19 | 0.04 | 0.44 | 0.48 | 0.22 | 0.49 |
| F- | 0.81 | − 0.02 | − 0.07 | 0.30 | − 0.34 | − 0.14 | 0.94 | 0.28 | − 0.01 | 0.11 |
| Cl- | 0.91 | − 0.11 | − 0.04 | 0.03 | 0.02 | 0.23 | 0.98 | 0.04 | 0.12 | 0.08 |
| NO2- | − 0.04 | − 0.06 | 0.93 | − 0.08 | 0.12 | − 0.01 | − 0.12 | 0.91 | 0.07 | 0.14 |
| Br- | − 0.04 | 0.01 | 0.41 | 0.29 | − 0.08 | 0.65 | 0.69 | 0.00 | 0.22 | 0.29 |
| NO3- | 0.82 | 0.37 | 0.21 | 0.03 | 0.00 | − 0.11 | 0.99 | − 0.01 | 0.05 | 0.00 |
| PO43- | 0.10 | 0.08 | − 0.19 | − 0.16 | 0.15 | 0.85 | 0.23 | 0.38 | − 0.67 | − 0.14 |
| SO42- | 0.97 | 0.10 | − 0.05 | − 0.02 | − 0.05 | − 0.13 | 0.99 | − 0.02 | 0.07 | − 0.03 |
| Total CO2 | 0.64 | 0.65 | − 0.02 | − 0.02 | 0.25 | 0.05 | 0.44 | 0.39 | 0.72 | − 0.07 |
| Date | − 0.12 | 0.14 | 0.22 | − 0.85 | − 0.07 | 0.16 | 0.07 | − 0.95 | − 0.05 | 0.14 |
| % of Variance | 43.03 | 12.19 | 10.22 | 9.81 | 7.81 | 7.26 | 52.17 | 13.85 | 11.72 | 10.69 |
| % of Variance (Cumulative) | **43.03** | **55.22** | **65.44** | **75.24** | **83.05** | **90.32** | **52.17** | **66.02** | **77.74** | **88.43** |

Bold indicates the cumulative is % Variance in cumulative

Extraction method: Principal Component Analysis

Rotation method: Varimax with Kaiser Normalization

[a]Rotation converged in 8 and 9 iterations

2. Total $CO_2$ was correlated with pH, alkalinity and major ions. The mean pH of rainwater in the study was observed to be in alkaline nature due to neutralizing ions such as $Ca^{2+}$ and $Mg^{2+}$; while only Shuaiba, industrial region reflected acidity. The temporal observation from 2005 to 2019 reflected an increasing trend of pH and alkalinity, which influenced the dissolution of $CO_2$.
3. Statistical correlation and PCA analysis inferred that the main contribution of $CO_2$ is from eroded crustal sources along with soil dust. Atmospheric dust from the inland contributed higher amounts of DIC and values greater than 800 µmoles/L were identified in the study region located in western parts and south of Kuwait Bay. Wind speed, its direction, temperature and sand storms also influenced the dissolution of $CO_2$ in rainwater.
4. DIC values in rainwater samples tend to be higher in the initial spells and reduced in the subsequent events. The total DIC flux derived from the rainwater during 2018 and 2019 were estimated to be 1,85,652 µmole/L and 39,362 µmoles/L.
5. A definite trend with a wide range of $pCO_2$ was observed in 2019 compared to 2018 and 2005 values. The $pCO_2$ of rainwater in Kuwait on comparison with global equilibrium values of $pCO_2$ of $CO_2$–$H_2O$, $CaCO_3$–$CO_2$–$H_2O$ were found to be lower except for one sample.
6. The spatial distribution of pH, DIC, $pCO_2$ and total $CO_2$ inferred that Shuaiba, an industrial region had acidic pH (5.69), which led to the highest $pCO_2$ (388.73 ppmV), while Ishbiliya, the residential region was noticed with alkaline pH containing high DIC and total $CO_2$ (1147.92µmole/L and 50.41 mg/L respectively).
7. DIC and $pCO_2$ values of the groundwater are generally higher than the sea and Bay waters. DIC in groundwater is mainly governed by lithology and dissolution temperature. The precipitation of carbonates releases $CO_2$ to the atmosphere.
8. Sea skin temperature and the $CO_2$ values along the sea-air interface play a key role in the carbon dynamics of the oceanic atmosphere. The $CO_2$ in the sea is governed by anthropogenic stress, residence time, amount of rainfall and wind speed.
9. The rainwater samples of GCC region had a definite ratio of $HCO_3^-/(Ca^{2+}+Mg^{2+})$ and a wide range of dissolved $CO_2$ depending on local conditions. The interplay of terrestrial $CO_2$ and oceanic $CO_2$ contributes to the atmospheric sink, which is later reflected in the total $CO_2$ of rainwater.

Overall, the study infers that the natural processes have a predominant control of $CO_2$ in the rainwater of Kuwait. The study has been carried out with the available data set for inorganic carbon values in the samples collected from 2018 November to 2019 December. The sample's organic carbon concentration and the stable carbon isotopes will also yield information on the sources and the atmospheric processes. Samples during a pandemic would be more significant to note if there has been a substantial variation in the dissolved $CO_2$ values in the rainwaters. The rainwater study in arid regions is scarce. The data on the $pCO_2$ variation in rainwater of other arid regions for and space would help assess the impact of aeolian dust and gasses. The sampling on each rain event and samples representing the same event in different time intervals can be focused on in future studies.

**Supplementary Information** The online version contains supplementary material available at https://doi.org/10.1007/s12665-022-10176-4.

**Acknowledgements** The authors would like to express their gratitude to the Kuwait Institute for Scientific Research (KISR), Kuwait. The authors would like to acknowledge the help, continuous support and encouragement received from Dr. Muhammad Al-Rashed, Executive Director, WRC, Dr. Khaled Hadi, Operations Director, WRC, and Dr. Yousef Al-Wazzan, Science and Technology Director, WRC during the successful execution of the study.

**Funding** The authors declare no competing financial interest.

## Declarations

**Conflict of interest** Not applicable.

**Data availability** Not applicable.

**Code availability** Not applicable.

**Ethical approval** Not applicable.

**Consent to participate** Not applicable.

**Consent for publication** Since this study is not attempting to republish or publish any third party or author's previously published material, this section does not apply.

## References

Ahmed AF, Singh RP, Elmubarak AH (1990) Chemistry of atmospheric precipitation at the Western Arabian Gulf Coast. Atmos Environ Part A Gen Top 24(12):2927–2934. https://doi.org/10.1016/0960-1686(90)90473-z

Alabdula'aly AI, Khan MA (2000) Chemistry of rain water in Riyadh, Saudi Arabia. Arch Environ Contam Toxicol 39(1):66–73. https://doi.org/10.1007/s002440010081

Ali A, Chidambaram S (2020) Assessment of trace inorganic contaminates in water and sediment to address its impact on common fish varieties along Kuwait Bay. Environ Geochem Health 43:1–29

Al-Khashman OA (2009) Chemical characteristics of rainwater collected at a western site of Jordan. Atmos Res 91:53–61

Almazroui M, Islam MN, Saeed S, Saeed F, Ismail M (2020) Future changes in climate over the Arabian Peninsula based on CMIP6 multimodel simulations. Earth Syst Environ 4:611–630

Al-Momani IF, Momani KA, Jaradat QM, Massadeh AM, Yousef YA, Alomary AA (2008) Atmospheric deposition of major and trace elements in Amman, Jordan. Environ Monit Assess 136:209–218
Al-Mutairi A, Smallbone A, Al-Salem S, Roskilly AP (2017) The first carbon atlas of the state of Kuwait. Energy 133:317–326
Al-Salem S (2015) Carbon dioxide ($CO_2$) emission sources in Kuwait from the downstream industry: critical analysis with a current and futuristic view. Energy 81:575–587
Arsene C, Olariu RI, Mihalopoulos N (2007) Chemical composition of rainwater in the northeastern Romania, Iasi region (2003–2006). Atmos Environ 41:9452–9467
Ashton I, Shutler J, Land P, Woolf DK, Quartly G (2016) A sensitivity analysis of the impact of rain on regional and global sea-air fluxes of $CO_2$. PLoS ONE 11:e0161105
ASTM (2009) American Standard Test method for the determination of dissolved alkali and alkaline earth cations and ammonium in water and wastewater by ion chromatography. D6919-09. https://webstore.ansi.org/standards/astm/astmd691909
Balasubramanian R, Victor T, Chun N (2001) Chemical and statistical analysis of precipitation in Singapore. Water Air Soil Pollut 130:451–456
Baltimoore C, Tudok R (2010) Relationships between energy and GNP. J Energy Dev 3:401–403
Bhandary H, Sabarathinam C, Al-Khalid A (2018) Occurrence of hypersaline groundwater along the coastal aquifers of Kuwait. Desalination 436:15–27
Bharti PK, Singh V, Tyagi PK (2017) Assessment of rainwater quality in industrial area of rural Panipat (Haryana), India. Arch Agric Environ Sci 2:219–223
Blain S, Quéguiner B, Armand L, Belviso S, Bombled B, Bopp L, Bowie A, Brunet C, Brussaard C, Carlotti F (2007) Effect of natural iron fertilization on carbon sequestration in the Southern Ocean. Nature 446:1070–1074
Bogan RA, Ohde S, Arakaki T, Mori I, McLeod CW (2009) Changes in rainwater pH associated with increasing atmospheric carbon dioxide after the industrial revolution. Water Air Soil Pollut 196:263–271
Bucchignani E, Mercogliano P, Panitz H-J, Montesarchio M (2018) Climate change projections for the Middle East-North Africa domain with COSMO-CLM at different spatial resolutions. Adv Clim Chang Res 9:66–80
Carroll D (1962) Rainwater as a chemical agent of geologic processes: a review. Citeseer
Cassar N, Laws EA, Bidigare RR, Popp BN (2004) Bicarbonate uptake by Southern Ocean phytoplankton. Glob Biogeochem Cycles. https://doi.org/10.1029/2003GB002116
Celle-Jeanton H, Travi Y, Loÿe-Pilot M-D, Huneau F, Bertrand G (2009) Rainwater chemistry at a Mediterranean inland station (Avignon, France): local contribution versus long-range supply. Atmos Res 91:118–126
Cerqueira MRF, Pinto MF, Derossi IN, Esteves WT, Santos MDR, Matos MAC, Lowinsohn D, Matos RC (2014) Chemical characteristics of rainwater at a southeastern site of Brazil. Atmos Pollut Res 5:253–261
Chidambaram S, Prasanna MV, Karmegam U, Singaraja C, Pethaperumal S, Manivannan R, Anandhan P, Tirumalesh K (2011) Significance of pCO 2 values in determining carbonate chemistry in groundwater of Pondicherry region, India. Front Earth Sci 5:197–206
Chidambaram S, Paramaguru P, Prasanna MV, Karmegam U, Manikandan S (2014) Chemical characteristics of coastal rainwater from Puducherry to Neithavasal, Southeastern coast of India. Environ Earth Sci 72:557–567
Chidambaram S, Bhandary H, Al-Khalid A (2020) Modeling of temperature governed saturation states and metal speciation in the marine waters of Kuwait Bay–concern to the desalination process. Desalin Water Treat 176:234–242
Chung S, Park H, Yoo J (2018) Variability of $pCO_2$ in surface waters and development of prediction model. Sci Total Environ 622:1109–1117
Cole JJ, Prairie YT, Caraco NF, McDowell WH, Tranvik LJ, Striegl RG, Duarte CM, Kortelainen P, Downing JA, Middelburg JJ (2007) Plumbing the global carbon cycle: integrating inland waters into the terrestrial carbon budget. Ecosystems 10:172–185
Czikowsky MJ, MacIntyre S, Tedford EW, Vidal J, Miller SD (2018) Effects of wind and buoyancy on carbon dioxide distribution and air-water flux of a stratified temperate lake. J Geophys Res Biogeosciences 123:2305–2322
De Gouw J, Jimenez JL (2009) Organic aerosols in the Earth's atmosphere. ACS Publications, Washington
Devaraj N, Chidambaram S, Gantayat RR, Thivya C, Thilagavathi R, Prasanna MV, Panda B, Adithya V, Vasudevan U, Pradeep K (2018) An insight on the speciation and genetical imprint of bicarbonate ion in the groundwater along K/T boundary, South India. Arab J Geosci 11:1–18
Devlin MJ, Breckels M, Graves CA, Barry J, Capuzzo E, Huerta FP, Al Ajmi F, Al-Hussain MM, LeQuesne WJ, Lyons BP (2019) Seasonal and temporal drivers influencing phytoplankton community in Kuwait marine waters: Documenting a changing landscape in the Gulf. Front Mar Sci 6:141
Dreybrodt W (2012) Processes in karst systems: physics, chemistry, and geology. Springer, Berlin
Dupré B, Dessert C, Oliva P, Goddéris Y, Viers J, François L, Millot R, Gaillardet J (2003) Rivers, chemical weathering and Earth's climate. CR Geosci 335:1141–1160
Ervens B, Turpin B, Weber R (2011) Secondary organic aerosol formation in cloud droplets and aqueous particles (aqSOA): a review of laboratory, field and model studies. Atmos Chem Phys 11:11069–11102
Facchini Cerqueira MR, Pinto MF, Derossi IN, Esteves WT, Rachid Santos MD, Costa Matos MA, Matos RC (2014) Chemical characteristics of rainwater at a southeastern site of Brazil. Atmos Pollut Res 5(2):253–261. https://doi.org/10.5094/apr.2014.031
Feely R, Takahashi T, Wanninkhof R, McPhaden M, Cosca C, Sutherland S, Carr ME (2006) Decadal variability of the air-sea CO2 fluxes in the equatorial Pacific Ocean. J Geophys Res Oceans. https://doi.org/10.1029/2005JC003129
Goldstein AH, Galbally IE (2007) Known and unexplored organic constituents in the earth's atmosphere. Environ Sci Technol 41:1514–1521
Gombert P (2002) Role of karstic dissolution in global carbon cycle. Glob Planet Change 33:177–184
Hadi K, Kumar US, Al-Senafy M, Bhandary H (2016) Environmental isotope systematics of the groundwater system of southern Kuwait. Environ Earth Sci 75:1–20
Hallquist M, Wenger JC, Baltensperger U, Rudich Y, Simpson D, Claeys M, Dommen J, Donahue N, George C, Goldstein A (2009) The formation, properties and impact of secondary organic aerosol: current and emerging issues. Atmos Chem Phys 9:5155–5236
Hendershot WH, Lalande H, Duquette M (1993) Soil reaction and exchangeable acidity. Soil Sampl Methods Anal 2
Henocq C, Boutin J, Reverdin G, Petitcolin F, Arnault S, Lattes P (2010) Vertical variability of near-surface salinity in the tropics: consequences for L-band radiometer calibration and validation. J Atmos Ocean Tech 27:192–209
Ho DT, Zappa CJ, McGillis WR, Bliven LF, Ward B, Dacey JW, Schlosser P, Hendricks MB (2004) Influence of rain on air-sea gas exchange: lessons from a model ocean. J Geophys Res Oceans. https://doi.org/10.1029/2003JC001806

Hoffman G, Prichard T, Maas E, Meyer J (1986) Irrigation water quality options for corn on saline, organic soils. Irrig Sci 7:265–275
Hutchinson GE (1957) A Treatise on limnology. Georgraphy, physics and chemistry, vol 1. Wiley, Hoboken
IAEA/GNIP (2014) Precipitation sampling guide (V2.02). http://www.iaea.org/water
Iavorivska L, Boyer EW, DeWalle DR (2016) Atmospheric deposition of organic carbon via precipitation. Atmos Environ 146:153–163
Iglesias-Rodriguez MD, Halloran PR, Rickaby RE, Hall IR, Colmenero-Hidalgo E, Gittins JR, Green DR, Tyrrell T, Gibbs SJ, von Dassow P (2008) Phytoplankton calcification in a high-$CO_2$ world. Science 320:336–340
IPCC (2013) Inter governmental Panel on Climate Change. http://www.climatechange2013.org/report/full-report. Accessed 2 Feb 2020
Ishii M, Saito S, Tokieda T, Kawano T, Matsumoto K, Inoue HY (2004) Variability of surface layer $CO_2$ parameters in the western and central equatorial Pacific. Global Environmental Changes in the Ocean and on Land. Shiyomi M, Kawahata H, Koizumi H, Tsuda A, Awaya Y (Eds.). TERRAPUB, Tokyo, pp. 59–94
Jones CD, Cox P, Huntingford C (2003) Uncertainty in climate'carbon-cycle projections associated with the sensitivity of soil respiration to temperature. Tellus b: Chem Phys Meteorol 55:642–648
Jurado E, Dachs J, Duarte CM, Simo R (2008) Atmospheric deposition of organic and black carbon to the global oceans. Atmos Environ 42:7931–7939
Kabwe L, Wilson G, Hendry J (2006) Field measurements of surface gas fluxes and surface-water conditions for mine waste rock management. 7th International conference on acid rock drainage (ICARD). Pp. 26–30
Kattan Z (2020) Factors affecting the chemical composition of precipitation in Syria. Environ Sci Pollut Res 27:28408–28428
Kempe S (1979) Carbon in the freshwater cycle. Glob Carbon Cycle 13:317–342
Ladouche B, Luc A, Nathalie D (2009) Chemical and isotopic investigation of rainwater in Southern France (1996–2002): potential use as input signal for karst functioning investigation. J Hydrol 367:150–164
Lara L, Artaxo P, Martinelli L, Victoria R, Camargo P, Krusche A, Ayers G, Ferraz E, Ballester M (2001) Chemical composition of rainwater and anthropogenic influences in the Piracicaba River Basin, Southeast Brazil. Atmos Environ 35:4937–4945
Leakey AD (2009) Rising atmospheric carbon dioxide concentration and the future of C4 crops for food and fuel. Proc R Soc B Biol Sci 276:2333–2343
Lerman A, Mackenzie FT (2005) $CO_2$ air–sea exchange due to calcium carbonate and organic matter storage, and its implications for the global carbon cycle. Aquat Geochem 11:345–390
Li P, Qian H, Wu J, Zhang Y, Zhang H (2013) Major ion chemistry of shallow groundwater in the Dongsheng Coalfield, Ordos Basin, China. Mine Water Environ 32(3):195–206. https://doi.org/10.1007/s10230-013-0234-8
Li P, Zhang Y, Yang N, Jing L, Yu P (2016) Major ion chemistry and quality assessment of groundwater in and around a mountainous tourist town of China. Expo Health 8(2):239–252. https://doi.org/10.1007/s12403-016-0198-6
Li P, Tian R, Liu R (2019) Solute geochemistry and multivariate analysis of water quality in the Guohua Phosphorite Mine, Guizhou Province, China. Expo Health 11(2):81–94. https://doi.org/10.1007/s12403-018-0277-y
Liu Z, Zhao J (2000) Contribution of carbonate rock weathering to the atmospheric CO 2 sink. Environ Geol 39:1053–1058
Liu Z, Li Q, Sun H, Wang J (2007) Seasonal, diurnal and storm-scale hydrochemical variations of typical epikarst springs in subtropical karst areas of SW China: soil $CO_2$ and dilution effects. J Hydrol 337:207–223
Liu Z, Dreybrodt W, Wang H (2010) A new direction in effective accounting for the atmospheric $CO_2$ budget: considering the combined action of carbonate dissolution, the global water cycle and photosynthetic uptake of DIC by aquatic organisms. Earth Sci Rev 99:162–172
Longinelli A, Lenaz R, Ori C, Selmo E (2005) Concentrations and. Tellus Ser B 57
Macpherson G, Roberts J, Blair J, Townsend M, Fowle D, Beisner K (2008) Increasing shallow groundwater $CO_2$ and limestone weathering, Konza Prairie, USA. Geochim Cosmochim Acta 72:5581–5599
Menz FC, Seip HM (2004) Acid rain in Europe and the United States: an update. Environ Sci Policy 7:253–265
Millot R, Érôme Gaillardet J, Dupré B, Allègre CJ (2003) Northern latitude chemical weathering rates: clues from the Mackenzie River Basin, Canada. Geochim Cosmochim Acta 67:1305–1329
Monastersky R (2013) Global carbon dioxide levels near worrisome milestone. Nat News 497:13
Moon S, Huh Y, Qin J, van Pho N (2007) Chemical weathering in the Hong (Red) River basin: rates of silicate weathering and their controlling factors. Geochim Cosmochim Acta 71:1411–1430
Moreda-Piñeiro J, Alonso-Rodríguez E, Moscoso-Pérez C, Blanco-Heras G, Turnes-Carou I, López-Mahía P, Prada-Rodríguez D (2014) Influence of marine, terrestrial and anthropogenic sources on ionic and metallic composition of rainwater at a suburban site (northwest coast of Spain). Atmos Env 88:30–38. https://doi.org/10.1016/j.atmosenv.2014.01.067
Mortatti J, Probst J-L (2003) Silicate rock weathering and atmospheric/soil $CO_2$ uptake in the Amazon basin estimated from river water geochemistry: seasonal and spatial variations. Chem Geol 197:177–196
Mukhopadhyay A, Al-Sulaimi J, Al-Awadi E, Al-Ruwaih F (1996) An overview of the Tertiary geology and hydrogeology of the northern part of the Arabian Gulf region with special reference to Kuwait. Earth Sci Rev 40:259–295
Munger JW (1982) Chemistry of atmospheric precipitation in the north-central United States: influence of sulfate, nitrate, ammonia and calcareous soil particulates. Atmos Environ 16:1633–1645
Naik PK, Mojica M, Ahmed F, Al-Mannai S (2017) Storm water injection in Bahrain: pilot studies. Arab J Geosci. https://doi.org/10.1007/s12517-017-3232-5
Naimabadi A, Shirmardi M, Maleki H, Teymouri P, Goudarzi G, Shahsavani A, Sorooshian A, Babaei AA, Mehrabi N, Baneshi MM, Zarei MR, Lababpour A, Ghozikali MG (2018) On the chemical nature of precipitation in a populated Middle Eastern Region (Ahvaz, Iran) with diverse sources. Ecotoxicol Environ Saf 163:558–566. https://doi.org/10.1016/j.ecoenv.2018.07.103
nasa.gov (2013) Global patterns of carbon dioxide. https://earthobservatory.nasa.gov/images/82142/global-patterns-of-carbon-dioxide
NOAA (2020) Rise of carbon dioxide unabated. https://research.noaa.gov/article/ArtMID/587/ArticleID/2636/Rise-of-carbon-dioxide-unabated
Nwaeze E, Ehiri RC (2017) The effect of increasing carbon dioxide level on rainwater: a numeric study of Nigeria. J Water Clim Change 8:40–47
Orlović-Leko P, Kozarac Z, Ćosović B, Strmečki S, Plavšić M (2010) Characterization of atmospheric surfactants in the bulk precipitation by electrochemical tools. J Atmos Chem 66:11–26
Panda B, Chidambaram S, Tirumalesh K, Ganesh N, Thivya C, Thilagavathi R, Venkatramanan S, Prasanna M, Devaraj N, Ramanathan A (2019) An integrated novel approach to understand the process of groundwater recharge in mountain and riparian zone aquifer system of Tamil Nadu, India. Aquat Geochem 25:137–159
Pathakoti M, Gaddamidi S, Gharai B, Sudhakaran Syamala P, Rao PVN, Choudhury SB, Raghavendra KV, Dadhwal VK (2018)

Influence of meteorological parameters on atmospheric $CO_2$ at Bharati, the Indian Antarctic research station. Polar Res 37:1442072
Peden ME, Skowron LM, McGurk FM (1979) Precipitation sample handling, analysis, and storage procedures. Ill State Water Surv
Pokavanich T, Alosairi Y (2014) Summer flushing characteristics of Kuwait Bay. J Coast Res 30:1066–1073
Qian H, Li P (2011) Mixing corrosion of $CaCO_3$ in natural waters. E J Chem 8(3):1124–1131. https://doi.org/10.1155/2011/891053
Qian H, Li P (2012) Proportion dependent mixing effects of $CaCO_3$ in natural waters. Asian J Chem 24(5):2257–2261
Rajendiran T, Sabarathinam C, Chandrasekar T, Keesari T, Senapathi V, Sivaraman P, Viswanathan PM, Nagappan G (2019) Influence of variations in rainfall pattern on the hydrogeochemistry of coastal groundwater—an outcome of periodic observation. Environ Sci Pollut Res 26:29173–29190
Rao P, Tiwari S, Matwale J, Pervez S, Tunved P, Safai P, Srivastava A, Bisht D, Singh S, Hopke P (2016) Sources of chemical species in rainwater during monsoon and non-monsoonal periods over two mega cities in India and dominant source region of secondary aerosols. Atmos Environ 146:90–99
Rastogi N, Sarin M (2005) Chemical characteristics of individual rain events from a semi-arid region in India: three-year study. Atmos Environ 39:3313–3323
Reay DS, Smith P, Hymus G, Sabine C (2007) New directions: the changing role of the terrestrial carbon sink in determining atmospheric $CO_2$ concentrations. Atmos Environ 41:5813–5815
Ren X, Li P, He X, Su F, Elumalai V (2021) Hydrogeochemical processes affecting groundwater chemistry in the central part of the Guanzhong Basin, China. Arch Environ Contam Toxicol 80(1):74–91. https://doi.org/10.1007/s00244-020-00772-5
Ridgwell A, Zeebe RE (2005) The role of the global carbonate cycle in the regulation and evolution of the Earth system. Earth Planet Sci Lett 234:299–315
Roger M, Brown F, Gabrielli W, Sargent F (2018) Efficient hydrogen-dependent carbon dioxide reduction by *Escherichia coli*. Curr Biol 28:140-145. e142
Rosegrant MW, Ringler C, Benson T, Diao X, Resnick D, Thurlow J, Torero M, Orden D (2006) Agriculture and achieving the millennium development goals. World Bank, Washington, DC, USA
Rousseaux CS, Gregg WW (2012) Climate variability and phytoplankton composition in the Pacific Ocean. J Geophys Res Oceans. https://doi.org/10.1029/2012JC008083
Sabarathinam C, Bhandary H, Al-Khalid A (2019) A geochemical analogy between the metal sources in Kuwait Bay and territorial sea water of Kuwait. Environ Monit Assess 191:1–19
Sabarathinam C, Bhandary H, Al-Khalid A (2020a) Tracing the evolution of acidic hypersaline coastal groundwater in Kuwait. Arab J Geosci 13:1–19
Sabarathinam C, Rashid T, Al-Qallaf H, Hadi K, Bhandary H (2020b) Paleoclimatic investigations using isotopic signatures of the Late Pleistocene-Holocene groundwater of the stratified aquifers in Kuwait. J Hydrol 588:125111
Sabine C, Feely R, Gruber N, Key R, Lee K, Bullister J, Wanninkhof R, Wong C, Wallace D, Tilbrook B (2004) The oceanic sink for anthropogenic $CO_2$. Science 305:367–371
Saleh SA, Taher T, Noaman A (2017) Manual for rooftop rainwater harvesting systems in the Republic of Yemen
Samayamanthula DR, Sabarathinam C, Alayyadhi NA (2021) Trace elements and their variation with pH in rain water in arid environment. Arch Environ Contam Toxicol 80:331–349
Saxena P, Hildemann LM, McMurry PH, Seinfeld JH (1995) Organics alter hygroscopic behavior of atmospheric particles. J Geophys Res Atmos 100:18755–18770
Senanayake N, Perera M, Weragoda A (2005) Acid rains and rains causing acidity of soils in Sri Lanka. AR-ACID RAIN 28
Shiklomanov IA (1993) World freshwater resources. Water in crisis: a guide to the World's fresh water resources. Oxford University Press, New York
Shimizu Y, Dejima S, Toyosada K (2013) $CO_2$ emission factor for rainwater and reclaimed water used in buildings in Japan. Water 5(2):394–404. https://doi.org/10.3390/w5020394
Shulman ML, Jacobson MC, Carlson RJ, Synovec RE, Young TE (1996) Dissolution behavior and surface tension effects of organic compounds in nucleating cloud droplets. Geophys Res Lett 23:277–280
Singh SK, Sarin M, France-Lanord C (2005) Chemical erosion in the eastern Himalaya: major ion composition of the Brahmaputra and δ13C of dissolved inorganic carbon. Geochim Cosmochim Acta 69:3573–3588
SMEWW (2017) Standard Methods for the Examination of Water and Waste Water. 23rd Edn. https://www.awwa.org/Store/Standard-Methods-for-the-Examination-of-Water-and-Wastewater-23rd-Edition/ProductDetail/65266295
Spracklen DV, Arnold SR, Sciare J, Carslaw KS, Pio C (2008) Globally significant oceanic source of organic carbon aerosol. Geophys Res Lett. https://doi.org/10.1029/2008GL033359
Stinner DH, Stinner BR, McCartney DA (1988) Effects of simulated acidic precipitation on plant—insect interactions in agricultural systems: corn and black cutworm larvae. Wiley Online Library
Tariq Rashid AA-H, Ebrahim S, Farhan M (2008) Characteristics and evaluation of urban rainwater in Kuwait. Kuwait J Sci Eng 35:27–146
Ternon J-F, Oudot C, Dessier A, Diverres D (2000) A seasonal tropical sink for atmospheric $CO_2$ in the Atlantic ocean: the role of the Amazon River discharge. Mar Chem 68:183–201
Tsigaridis K, Kanakidou M (2003) Global modelling of secondary organic aerosol in the troposphere: a sensitivity analysis. Atmos Chem Phys 3:1849–1869
Turk D, Zappa CJ, Meinen CS, Christian JR, Ho DT, Dickson AG, McGillis WR (2010) Rain impacts on $_{CO2}$ exchange in the western equatorial Pacific Ocean. Geophys Res Lett. https://doi.org/10.1029/2010GL045520
USGA (2020) United States Geological survey (USGS). http://www.usgs.gov
Voiland A (2019) Historic floods inundate nebraska. NASA Earth Observatory
Wang F, Wang Y (2006) Human impact on historical change of $CO_2$ degassing flux in the Changjiang River, China. Chin J Geochem 25:277–277
Wu L, Huh Y, Qin J, Du G, van Der Lee S (2005) Chemical weathering in the Upper Huang He (Yellow River) draining the eastern Qinghai-Tibet Plateau. Geochim Cosmochim Acta 69:5279–5294
Wu W, Xu S, Yang J, Yin H (2008) Silicate weathering and $CO_2$ consumption deduced from the seven Chinese rivers originating in the Qinghai-Tibet Plateau. Chem Geol 249:307–320
Wu J, Li P, Qian H, Duan Z, Zhang X (2014) Using correlation and multivariate statistical analysis to identify hydrogeochemical processes affecting the major ion chemistry of waters: case study in Laoheba phosphorite mine in Sichuan, China. Arab J Geosci 7(10):3973–3982. https://doi.org/10.1007/s12517-013-1057-4
Wu J, Li P, Wang D, Ren X, Wei M (2020) Statistical and multivariate statistical techniques to trace the sources and affecting factors of groundwater pollution in a rapidly growing city on the Chinese Loess Plateau. Hum Ecol Risk Assess 26(6):1603–1621. https://doi.org/10.1080/10807039.2019.1594156
Yang H, Xing Y, Xie P, Ni L, Rong K (2008) Carbon source/sink function of a subtropical, eutrophic lake determined from an overall mass balance and a gas exchange and carbon burial balance. Environ Pollut 151:559–568

Yassin MF, Almutairi SK, Al-Hemoud A (2018) Dust storms backward Trajectories' and source identification over Kuwait. Atmos Res 212:158–171

Zappa CJ, Ho DT, McGillis WR, Banner ML, Dacey JW, Bliven LF, Ma B, Nystuen J (2009) Rain-induced turbulence and air-sea gas transfer. J Geophys Res Oceans. https://doi.org/10.1029/2008JC005008

Zhang DD, Peart M, Jim CY, He Y, Li B, Chen J (2003) Precipitation chemistry of Lhasa and other remote towns. Tibet Atmos Environ 37:231–240

Ziska LH (2008) Rising atmospheric carbon dioxide and plant biology: the overlooked paradigm. DNA Cell Biol 27:165–172

Zondervan I (2007) The effects of light, macronutrients, trace metals and $CO_2$ on the production of calcium carbonate and organic carbon in coccolithophores—a review. Deep-Sea Res II 54:521–537